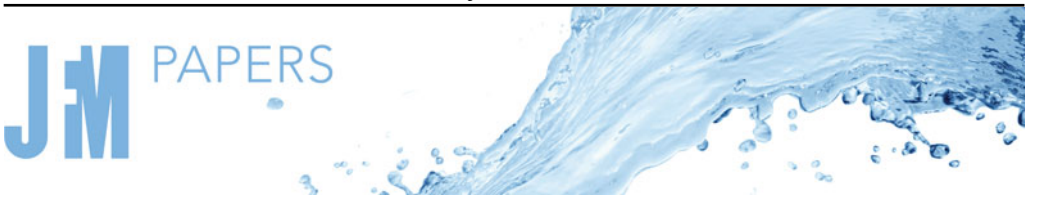
J. Fluid Mech. (2026), *vol.* 1045, A46, doi:10.1017/jfm.2026.12065



A consistent phase-averaged model of the interactions between surface gravity waves and currents

Jacques Vanneste[1] **and William R. Young**[2]

[1]School of Mathematics and Maxwell Institute for Mathematical Sciences, University of Edinburgh, Edinburgh, EH9 3FD, UK

[2]Scripps Institution of Oceanography, University of California at San Diego, La Jolla, CA 92093-0213, USA

Corresponding author: Jacques Vanneste, j.vanneste@ed.ac.uk

(Received 23 February 2026 UTC; revised 11 June 2026 UTC; accepted 25 August 2026 UTC)

We formulate a model of the two-way interactions between surface gravity waves and ocean currents. The model couples the transport of wave action in the four-dimensional (horizontal) position–wavevector phase space with the Craik–Leibovich system for the currents. Coupling is via the Doppler shift in the dispersion relation governing action transport, and wave pseudomomentum in the Craik–Leibovich system. The velocity in the Doppler shift is a vertical integral of the Lagrangian mean velocity of the currents, with a weight that is consistent with the vertical structure of the pseudomomentum. This consistency ensures conservation of momentum and energy in the coupled wave–current system. The conservation properties of the wave–current model stem from an underlying variational structure. We derive this structure from that of the rotating Euler equations for an incompressible fluid with free surface by introducing a Lagrangian wave–mean decomposition, making simplifying approximations, and Whitham averaging. The wave–mean decomposition is constructed such that the Lagrangian mean velocity is non-divergent and satisfies a rigid-lid boundary condition. We apply the wave–current model to the problem of generation of inertial oscillations by surface waves originally considered by Hasselmann.

Key words: wave-turbulence interactions, variational methods, surface gravity waves

© The Author(s), 2026. Published by Cambridge University Press. This is an Open Access article, distributed under the terms of the Creative Commons Attribution licence (https://creativecommons.org/licenses/by/4.0/), which permits unrestricted re-use, distribution and reproduction, provided the original article is properly cited.

https://doi.org/10.1017/jfm.2026.12065 Published online by Cambridge University Press

1. Introduction

Two-way interactions between ocean currents and high-frequency surface gravity waves dominate sea-surface dynamics. The slow, phase-averaged evolution of the wave field can be modelled with the wave-action transport equation (2.1), governing dynamics in position–wavenumber phase space. The action transport equation captures the effect of currents on waves, namely advection and refraction, through a Doppler-shift term in the dispersion relation. On the other hand, the effect of waves on currents via the Stokes–Coriolis force (Hasselmann 1970; Huang 1979) and the vortex force is modelled by the Craik–Leibovich equation (Craik & Leibovich 1976; Leibovich 1980) and its extensions (McWilliams *et al.* 2004; Ardhuin *et al.* 2008; McWilliams 2022). Both forces depend on wave action through the Stokes velocity $\boldsymbol{u}^S$. Doppler-shift and wave-averaged forces are the non-dissipative wave–mean-flow interactions by which energy and momentum are exchanged between waves and currents.

Although this exchange can proceed in both directions, a popular simplification considers the wave field for prescribed currents. This simplification underpins recent work on the action transport equation (Villas Bôas *et al.* 2020; Villas Bôas & Young 2020; Wang *et al.* 2023, 2025; Resseguier *et al.* 2024; Hell *et al.* 2025) and the vast literature based on ray tracing (e.g. White & Fornberg 1998; Gallet & Young 2014). Likewise, many studies solve the Craik–Leibovich equation (2.8) with prescribed Stokes velocity $\boldsymbol{u}^S(z)$ (e.g. Skyllingstad & Denbo 1995; McWilliams *et al.* 1997; Seshasayanan & Gallet 2019; Wagner *et al.* 2021, 2023). Prescription of either waves or currents severs the wave–mean-flow interaction problem into non-communicating halves.

Coupled models have emerged in the last decade. Driven by the demands of operational oceanography, established wave models based on the action transport equation are paired with ocean circulation models (e.g. Breivik *et al.* 2015; Clementi *et al.* 2017; Couvelard *et al.* 2020; Sun *et al.* 2023; Porcile *et al.* 2024). This *a posteriori* coupling does not treat the wave-action and Craik–Leibovich equations in a consistent manner. As a result, the conservation laws of energy and momentum are damaged.

Here we formulate a consistent model describing the joint evolution of waves and currents (§ 2). Main elements of this framework are familiar: currents enter the action transport equation via the Doppler shift $\boldsymbol{k}\cdot\boldsymbol{\mathcal{U}}$ in the dispersion relation. But it is not obvious how the Doppler velocity $\boldsymbol{\mathcal{U}}$ relates to the current in the Craik–Leibovich system. We show that taking $\boldsymbol{\mathcal{U}}$ to be a suitable (wavenumber-dependent) weighted vertical average of the Lagrangian mean velocity $\boldsymbol{u}^L$ leads to a coupled model conserving energy and momentum (§ 3).

The coupled model is consistent and enjoys conservation properties because of an underlying variational formulation. We obtain this formulation from a variational form of the rotating Euler equations with free surface by making a series of approximations: wave–mean decomposition, linear-wave ansatz and Whitham averaging (§ 4). This applies the approach pioneered by Dewar (1970) and Bretherton (1971) for hydromagnetic and acoustic waves to surface gravity waves. The approach was subsequently used by Grimshaw (1984), Gjaja & Holm (1996) and Salmon (2016) for internal and Poincaré waves, and by Salmon (2020) and Pizzo & Salmon (2021) for surface waves interacting with a two-dimensional quasigeostrophic flow (see also Xie & Vanneste 2015; Holm *et al.* 2023). Our treatment follows most closely that of Dewar (1970) in relying on an Eulerian variational formulation and allowing for a broad wave spectrum. We exploit arbitrariness in the separation between mean current and waves to constrain the Lagrangian mean velocity to be divergence free, following Soward & Roberts (2010), and the mean free

https://doi.org/10.1017/jfm.2026.12065 Published online by Cambridge University Press

surface to be flat. A distinguishing feature of our model compared with previous work is that the Doppler velocity $\boldsymbol{\mathcal{U}}$ is a weighted vertical integral of $\boldsymbol{u}^L$ rather than $\boldsymbol{u}^L$ itself because the sea surface is a waveguide.

The exact conservation of energy and momentum in the absence of forcing and dissipation for the coupled model of § 2 is key to understanding wave–current interactions. Without a conserved energy it is impossible to decide on the 'best' definition of mean kinetic energy, whether the Lagrangian mean kinetic energy $|\boldsymbol{u}^L|^2/2$ or its Eulerian counterpart $|\boldsymbol{u}^E|^2/2$, neither of which are conserved according to the Craik–Leibovich equation alone. Without a consistently coupled wave-action equation, the non-conservative terms in the energy equation of the currents can always be attributed to energy exchanges with the waves. The consistent wave–current model (CWCM) in § 2 answers questions that are inherently ambiguous when examined with either prescribed Stokes velocity in the Craik–Leibovich equation or prescribed currents in the action equation. For example, with a complete understanding of energy conservation, we show in §§ 3 and 5 that the conserved energy involves the Lagrangian kinetic energy (LKE) $|\boldsymbol{u}^L|^2/2$ rather than its Eulerian counterpart $|\boldsymbol{u}^E|^2/2$.

As a simple application, we revisit the generation of inertial oscillations by surface waves considered by Hasselmann (1970) (§ 5). We replace Hasselmann's prescribed Stokes velocity $\boldsymbol{u}^S$ by a prescribed forcing of the action transport equation. Prescribed forcing of the action represents the effect of wind more directly than prescription of $\boldsymbol{u}^S$ in the Craik–Leibovich equation. The current dynamics obtained with the wave–current model is identical to that of Hasselmann but the energetics of the process is now clear: the energy of the inertial oscillations is not drawn from the wave energy but instead requires additional wind work.

2. A CWCM

The coupled model summarised in this section – referred to as CWCM – follows from the application of Hamilton's principle to an approximate Lagrangian, given in (4.23). The derivation of this approximate Lagrangian, starting from the exact Lagrangian for rotating incompressible flow in (4.2), is technically demanding. Instead, it is economical to first present the CWCM, then verify its conservation laws (§ 3).

The phase-averaged wave field is characterised by the wave-action density $\mathcal{N}(\boldsymbol{x}, \boldsymbol{k})$. Our notation is that $\boldsymbol{k} = (k, l) = (k_1, k_2)$ and $\boldsymbol{x} = (x, y) = (x_1, x_2)$ are horizontal vectors; unless emphasis is required we do not indicate dependence of various fields on time t. We indicate functions of the phase space variables $(\boldsymbol{x}, \boldsymbol{k})$ using calligraphics, e.g. the action density $\mathcal{N}(\boldsymbol{x}, \boldsymbol{k})$ and also $\boldsymbol{\mathcal{U}}(\boldsymbol{x}, \boldsymbol{k})$ and $\boldsymbol{\mathcal{C}}(\boldsymbol{x}, \boldsymbol{k})$ below. We make exceptions for fields traditionally denoted by Greek letters, e.g. the absolute and intrinsic frequencies $\Omega(\boldsymbol{x}, \boldsymbol{k})$ and $\sigma(\boldsymbol{x}, \boldsymbol{k})$ below. The action density $\mathcal{N}(\boldsymbol{x}, \boldsymbol{k})$ is the phase-space energy density divided by intrinsic frequency $\sigma(\boldsymbol{x}, \boldsymbol{k})$ and, in our convention, divided by the constant fluid density ρ.

The evolution of the phase-averaged wave field is determined by the action balance equation:

$$\partial_t \mathcal{N} + \boldsymbol{\nabla}_{\boldsymbol{k}}\, \Omega \cdot \boldsymbol{\nabla}_{\boldsymbol{x}} \mathcal{N} - \boldsymbol{\nabla}_{\boldsymbol{x}}\, \Omega \cdot \boldsymbol{\nabla}_{\boldsymbol{k}}\, \mathcal{N} = \mathcal{N}^{\circ} \tag{2.1}$$

(e.g. Komen *et al.* 1996; Janssen 2004; Holthuijsen 2010). Here $\mathcal{N}^{\circ}$ on the right-hand side of (2.1) denotes sources and sinks of wave action and nonlinear interactions between waves. We consider water with depth $d(\boldsymbol{x})$ so that the wave frequency in (2.1) is

$$\Omega(\boldsymbol{x}, \boldsymbol{k}) = \sigma(\boldsymbol{x}, \kappa) + \boldsymbol{k} \cdot \boldsymbol{\mathcal{U}}(\boldsymbol{x}, \kappa), \tag{2.2}$$

https://doi.org/10.1017/jfm.2026.12065 Published online by Cambridge University Press

where

$$\sigma(\boldsymbol{x}, \kappa) = \sqrt{g\kappa \tanh(\kappa\, d(\boldsymbol{x}))}, \quad \text{with} \quad \kappa = |\boldsymbol{k}| = \sqrt{k^2 + l^2}, \tag{2.3}$$

is the intrinsic frequency. In (2.2) the Doppler shift $\boldsymbol{k} \cdot \boldsymbol{\mathcal{U}}$ is based on the 'Doppler velocity'

$$\boldsymbol{\mathcal{U}}(\boldsymbol{x}, \kappa) \stackrel{\text{def}}{=} \int_{-d(\boldsymbol{x})}^{0} \boldsymbol{u}^L(\boldsymbol{x}, z)\, Q(\boldsymbol{x}, z, \kappa)\, \mathrm{d}z, \tag{2.4}$$

where $\boldsymbol{u}^L(\boldsymbol{x}, z)$ is the three-dimensional Lagrangian mean velocity and

$$Q(\boldsymbol{x}, z, \kappa) \stackrel{\text{def}}{=} \frac{2\kappa \cosh(2\kappa(z + d(\boldsymbol{x})))}{\sinh(2\kappa d(\boldsymbol{x}))} \tag{2.5}$$

is such that

$$\int_{-d(\boldsymbol{x})}^{0} Q(\boldsymbol{x}, z, \kappa)\, \mathrm{d}z = 1. \tag{2.6}$$

Because $\boldsymbol{k}$ is a horizontal vector, the vertical component of $\boldsymbol{\mathcal{U}}$ plays no role in (2.1)–(2.2) or in the sequel.

In the derivation of the CWCM in § 4 the 'vertical averaging kernel', $Q(\boldsymbol{x}, z, \kappa)$ in (2.5), is produced by inserting the linear-wave ansatz (4.13) into a Lagrangian and Whitham-averaging. The resulting dispersion relation (2.2) with (2.4)–(2.5) is also obtained by Kirby & Chen (1989) as an approximation to the dispersion relation of finite-depth waves propagating in a vertically sheared current. In deep water,

$$Q(\boldsymbol{x}, z, \kappa) = 2\kappa\, \mathrm{e}^{2\kappa z}, \tag{2.7}$$

as originally obtained by Stewart & Joy (1974).

The dispersion relation with (2.4) and (2.5) is used by Ardhuin *et al.* (2008) in their extension of the Craik–Leibovich system. In all these earlier instances, the Doppler velocity involves the Eulerian mean velocity $\boldsymbol{u}^E$ instead of the Lagrangian mean velocity $\boldsymbol{u}^L$ in (2.4). In contrast, the systematic analysis of small-amplitude single wavetrains in deep water using Lagrangian coordinates leads to the Doppler velocity in the form (2.4) with $d \to \infty$ (Abrashkin & Pelinovsky 2017, 2018; Pizzo *et al.* 2023).

The validity of the dispersion relation (2.2) requires the shear to be weak and is ensured provided that $|\partial_z \boldsymbol{u}_h^L| \ll \sigma$, with $\boldsymbol{u}_h^L$ the horizontal Lagrangian mean velocity (cf. Banihashemi & Kirby 2019).

The evolution of the Lagrangian mean current $\boldsymbol{u}^L(\boldsymbol{x}, z) = (u^L, v^L, w^L)$ is determined by the Craik–Leibovich system

$$\partial_t(\boldsymbol{u}^L - \mathbf{p}) + (\boldsymbol{f} + \boldsymbol{\nabla} \times (\boldsymbol{u}^L - \mathbf{p})) \times \boldsymbol{u}^L + \boldsymbol{\nabla}\pi = \boldsymbol{u}^\circ, \tag{2.8}$$

$$\boldsymbol{\nabla} \cdot \boldsymbol{u}^L = 0,$$

where $\boldsymbol{\nabla} = (\boldsymbol{\nabla}_{\boldsymbol{x}}, \partial_z)$ is the three-dimensional spatial gradient. In (2.8) $\boldsymbol{f}$ is a constant vector; we do not make the traditional approximation. Coupling between the action conservation (2.1) and the Lagrangian mean velocity $\boldsymbol{u}^L(\boldsymbol{x}, z)$ is via the pseudomomentum

$$\mathbf{p}(\boldsymbol{x}, z) \stackrel{\text{def}}{=} \iint Q(\boldsymbol{x}, z, \kappa) \mathcal{N}(\boldsymbol{x}, \boldsymbol{k}) \boldsymbol{k}\, \mathrm{d}\boldsymbol{k}. \tag{2.10}$$

https://doi.org/10.1017/jfm.2026.12065 Published online by Cambridge University Press

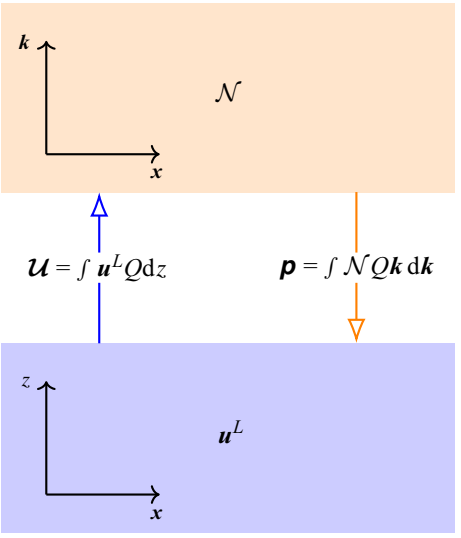


Figure 1. Schematic of the CWCM: the dynamical variables are the action density $\mathcal{N}(\boldsymbol{x}, \boldsymbol{k})$ and the current Lagrangian mean velocity $\boldsymbol{u}^L(\boldsymbol{x}, z)$. They are coupled through the pseudomomentum $\mathbf{p}(\boldsymbol{x}, z)$ and the weighted horizontal velocity $\boldsymbol{\mathcal{U}}(\boldsymbol{x}, \kappa)$ that appears in the surface wave dispersion relation.

Pseudomomentum $\mathbf{p}(\boldsymbol{x}, z)$ is a horizontal vector. Integrating (2.10) over z and using (2.6) produces the important identity

$$\int_{-d(\boldsymbol{x})}^{0} \mathbf{p}(\boldsymbol{x}, z)\, \mathrm{d}z = \iint \mathcal{N}(\boldsymbol{x}, \boldsymbol{k}) \boldsymbol{k}\, \mathrm{d}\boldsymbol{k}. \tag{2.11}$$

The Craik–Leibovich system is completed with the $z = 0$ rigid-lid boundary condition on the Lagrangian mean vertical velocity

$$w^L(x, y, 0, t) = 0, \tag{2.12}$$

and the no-normal-flow bottom boundary condition

$$w^L + \boldsymbol{u}^L \cdot \boldsymbol{\nabla}_{\boldsymbol{x}} d = 0 \quad \text{at} \quad z = -d(\boldsymbol{x}). \tag{2.13}$$

The rigid-lid boundary condition ensures that (2.8) and (2.9) does not have wave solutions, i.e. waves are filtered from the wave-averaged equations.

The system in (2.1) through (2.13) is the dynamical core of the CWCM. Additional processes, such as forcing, dissipation and wave–wave interactions, can be added by specification of the right-hand sides $\mathcal{N}^\circ$ and $\boldsymbol{u}^\circ$ of (2.1) and (2.8). The model combines the dynamics of the action in the four-dimensional $(\boldsymbol{x}, \boldsymbol{k})$ phase space with Craik–Leibovich dynamics in the three-dimensional $(\boldsymbol{x}, z)$ physical space. The two components of the model interact via the pseudomomentum $\mathbf{p}(\boldsymbol{x}, z)$ and the horizontal Doppler velocity $\boldsymbol{\mathcal{U}}(\boldsymbol{x}, \kappa)$, both of which involve the weight function $Q(\boldsymbol{x}, z, \kappa)$. This is illustrated in figure 1.

The CWCM uses the Lagrangian mean velocity $\boldsymbol{u}^L$ and the pseudomomentum $\mathbf{p}$; the Stokes velocity $\boldsymbol{u}^S$ and the Eulerian mean velocity $\boldsymbol{u}^E$ do not appear. For approximately irrotational waves, as assumed in the derivation in § 4, $\boldsymbol{u}^S \approx \mathbf{p}$. Thus, one can compare the CWCM with other formulations of the mean momentum equation that employ $\boldsymbol{u}^S$ and $\boldsymbol{u}^E = \boldsymbol{u}^L - \boldsymbol{u}^S \approx \boldsymbol{u}^L - \mathbf{p}$ as main variables (e.g. Craik & Leibovich 1976; McWilliams *et al.* 2004; Suzuki & Fox-Kemper 2016).

https://doi.org/10.1017/jfm.2026.12065 Published online by Cambridge University Press

An unfamiliar feature of the CWCM is that the Lagrangian mean $\boldsymbol{u}^L$, depth-weighted in (2.4) with the kernel $Q(\boldsymbol{x}, z, \kappa)$, is the Doppler velocity $\boldsymbol{\mathcal{U}}(\boldsymbol{x}, \kappa)$ in the dispersion relation (2.2). Because $\boldsymbol{\mathcal{U}}$ depends on κ the group velocity is

$$\boldsymbol{\mathcal{C}}(\boldsymbol{x}, \boldsymbol{k}) = \boldsymbol{\nabla}_{\boldsymbol{k}}\Omega = \mathcal{G}(\boldsymbol{x}, \boldsymbol{k})\boldsymbol{k} + \boldsymbol{\mathcal{U}}(\boldsymbol{x}, \kappa), \tag{2.14}$$

where

$$\mathcal{G}(\boldsymbol{x}, \boldsymbol{k}) \stackrel{\text{def}}{=} \frac{1}{\kappa}\frac{\partial\sigma}{\partial\kappa} + \frac{\boldsymbol{k}}{\kappa}\cdot\frac{\partial\boldsymbol{\mathcal{U}}}{\partial\kappa}. \tag{2.15}$$

Banihashemi *et al.* (2017) and Banihashemi & Kirby (2019) have drawn attention to κ-dependence of the current in the wave-action conservation and the peculiar term involving $\partial\boldsymbol{\mathcal{U}}/\partial\kappa$ in $\mathcal{G}$.

For reference we record alternative equivalent forms of the Craik–Leibovich equation (2.8). Andrews & McIntyre (1978) and Leibovich (1980) favour the form that emerges directly from the application of Hamilton's principle in § 4,

$$\left(\partial_t + u_j^L\partial_j\right)\left(u_i^L - \mathsf{p}_i\right) + \left(u_j^L - \mathsf{p}_j\right)\partial_i u_j^L + (\boldsymbol{f}\times\boldsymbol{u}^L)_i + \partial_i\hat{\pi} = u_i^\circ. \tag{2.16}$$

In (2.16) italic indices i and j run from 1 to 3, ∂_i is shorthand for $\partial/\partial x_i$ and

$$\hat{\pi} \stackrel{\text{def}}{=} \pi + \mathbf{p}\cdot\boldsymbol{u}^L - |\boldsymbol{u}^L|^2. \tag{2.17}$$

Another equivalent form is

$$\partial_t u_i^L - \partial_t\mathsf{p}_i - \mathsf{p}_j\partial_i u_j^L + \partial_j\left(u_i^L u_j^L - \mathsf{p}_i u_j^L\right) + (\boldsymbol{f}\times\boldsymbol{u}^L)_i + \partial_i\tilde{\pi} = u_i^\circ, \tag{2.18}$$

where

$$\tilde{\pi} = \pi + \mathbf{p}\cdot\boldsymbol{u}^L - \tfrac{1}{2}|\boldsymbol{u}^L|^2. \tag{2.19}$$

The form in (2.18) is useful in the discussion of momentum conservation in § 3.2. Suzuki & Fox-Kemper (2016) present five alternative versions of the Craik–Leibovich equation with $\boldsymbol{u}^E$ or $\boldsymbol{u}^L$ as the primary velocity. All versions follow from (2.8), (2.16) or (2.18) on using $\boldsymbol{u}^L - \mathbf{p} = \boldsymbol{u}^E$ and $\mathbf{p} = \boldsymbol{u}^S$.

3. Conservation laws

The CWCM in § 2 conserves action, mass, energy, momentum, circulation and potential vorticity. According to (2.1), the action density $\mathcal{N}(\boldsymbol{x}, \boldsymbol{k})$ is transported by the non-divergent phase-space velocity $(\boldsymbol{\nabla}_{\boldsymbol{k}}\Omega, -\boldsymbol{\nabla}_{\boldsymbol{x}}\Omega)$. The corresponding conservative form of (2.1) is

$$\partial_t\mathcal{N} + \boldsymbol{\nabla}_{\boldsymbol{x}}\cdot(\mathcal{N}\boldsymbol{\nabla}_{\boldsymbol{k}}\Omega) - \boldsymbol{\nabla}_{\boldsymbol{k}}\cdot(\mathcal{N}\boldsymbol{\nabla}_{\boldsymbol{x}}\Omega) = \mathcal{N}^\circ. \tag{3.1}$$

If $F(\cdot)$ is any function, multiplying (3.1) by the derivative $F'(\mathcal{N}(\boldsymbol{x}, \boldsymbol{k}))$ shows that

$$\iint F(\mathcal{N}(\boldsymbol{x}, \boldsymbol{k}))\,\mathrm{d}\boldsymbol{x}\mathrm{d}\boldsymbol{k} \tag{3.2}$$

is conserved when $\mathcal{N}^\circ = 0$. The conservative form in (3.1) is also the most convenient for forming $\boldsymbol{k}$-weighted moments of the action equation, e.g. as in (3.3).

3.1. *Mass conservation*

The Lagrangian average used in the formulation above, with a non-divergent $\boldsymbol{u}^L$ in (2.9), is not the generalised Lagrangian mean (GLM) of Andrews & McIntyre (1978): in GLM,

https://doi.org/10.1017/jfm.2026.12065 Published online by Cambridge University Press

$\boldsymbol{u}^L$ has non-zero divergence (McIntyre 1988; Ardhuin *et al.* 2008). Instead, we use the Lagrangian mean of Soward & Roberts (2010) (written as glm in Soward & Roberts (2010)) which has a non-divergent Lagrangian mean velocity (Vanneste & Young 2022).

(Mass is conserved by GLM: with non-zero $\boldsymbol{\nabla}\cdot\boldsymbol{u}^L$ there is a Lagrangian density variable – denoted $\tilde{\rho}$ in Andrews & McIntyre (1978) – ensuring mass conservation. Our decision to use the Lagrangian mean of Soward & Roberts (2010), with exact $\boldsymbol{\nabla}\cdot\boldsymbol{u}^L=0$, avoids the additional ρ-variable.)

3.2. *Momentum conservation*

We start with the vertically integrated pseudomomentum equation obtained by forming $\iint(3.1)\boldsymbol{k}\,\mathrm{d}\boldsymbol{k}$:

$$\partial_t\iint\mathcal{N}(\boldsymbol{x},\boldsymbol{k})k_\alpha\,\mathrm{d}\boldsymbol{k}+\partial_\beta\iint\mathcal{C}_\beta k_\alpha\mathcal{N}\mathrm{d}\boldsymbol{k}+\iint\mathcal{N}\partial_\alpha\Omega\,\mathrm{d}\boldsymbol{k}=\iint k_\alpha\mathcal{N}^\circ\,\mathrm{d}\boldsymbol{k}. \tag{3.3}$$

In (3.3) the Greek indices α and β run from 1 to 2 and ∂_α and ∂_β denote derivatives with respect to x_α, e.g. $\partial_\alpha=\partial/\partial x_\alpha$. The group velocity, $\mathcal{C}_\beta$ above, is defined in (2.14). With pseudomomentum $\mathsf{p}(\boldsymbol{x},z)$ defined in (2.10), the first term in (3.3) is ∂_t applied to the total vertical integral of $\mathsf{p}(\boldsymbol{x},z)$. The third term in (3.3), involving $\partial_\alpha\Omega$, is transformed by switching the order of $\boldsymbol{k}$- and z-integrals; see Appendix A for details. These manipulations bring (3.3) to the form

$$\partial_t\int\mathsf{p}_\alpha\,\mathrm{d}z+\partial_\beta\iint\mathcal{C}_\beta k_\alpha\mathcal{N}\,\mathrm{d}\boldsymbol{k}+\int\mathsf{p}_\beta\partial_\alpha u^L_\beta\,\mathrm{d}z+\iint\frac{\partial\Omega}{\partial d}\mathcal{N}\mathrm{d}\boldsymbol{k}\,\partial_\alpha d=\iint k_\alpha\mathcal{N}^\circ\,\mathrm{d}\boldsymbol{k}. \tag{3.4}$$

Above and hereafter, we lighten notation by suppressing the limits $-d(\boldsymbol{x})$ and 0 on vertical integrals. In writing the derivative $\partial\Omega/\partial d$ we abuse notation slightly by treating Ω as a function of d rather than $\boldsymbol{x}$ as in (2.2). The interpretation is clear from the explicit dependence of σ and $\boldsymbol{\mathcal{U}}$ (via Q) on d in (2.3) and (2.4)–(2.5). We give an explicit expression for $\partial\Omega/\partial d$ in (A3) and (A8).

Turning to the Craik–Leibovich equation, the vertical integral of the horizontal components of (2.18) is

$$\begin{aligned}\partial_t\int u^L_\alpha\,\mathrm{d}z-\partial_t\int\mathsf{p}_\alpha\mathrm{d}z-\int\mathsf{p}_\beta\partial_\alpha u^L_\beta\,\mathrm{d}z+\partial_\beta\int u^L_\alpha u^L_\beta-\mathsf{p}_\alpha u^L_\beta\,\mathrm{d}z\\+\Big(\int\boldsymbol{f}\times\boldsymbol{u}^L\,\mathrm{d}z\Big)_\alpha+\partial_\alpha\int\tilde{\pi}\,\mathrm{d}z-[\tilde{\pi}]_{-d}\,\partial_\alpha d=\int u^\circ_\alpha\,\mathrm{d}z,\end{aligned} \tag{3.5}$$

where $[\,\cdot\,]_{-d}$ denotes evaluation at $z=-d$, e.g. $[\tilde{\pi}]_{-d}=\tilde{\pi}(\boldsymbol{x},-d(\boldsymbol{x}))$. Terms stemming from the commutation of ∂_β with the vertical integral vanish on using the boundary conditions (2.12) and (2.13). The sole remaining boundary contribution is the topographic form stress $[\tilde{\pi}]_{-d}\,\partial_\alpha d$ in (3.5).

Adding (3.4) and (3.5) cancels the terms

$$\partial_t\int\mathsf{p}_\alpha\,\mathrm{d}z+\int\mathsf{p}_\beta\partial_\alpha u^L_\beta\,\mathrm{d}z, \tag{3.6}$$

https://doi.org/10.1017/jfm.2026.12065 Published online by Cambridge University Press

leaving

$$\partial_t \int u^L_\alpha \,\mathrm{d}z + \partial_\beta \left(\int u^L_\alpha u^L_\beta - \mathsf{p}_\alpha u^L_\beta \,\mathrm{d}z + \iint k_\alpha \mathcal{C}_\beta \mathcal{N} \mathrm{d}\boldsymbol{k} \right) + \Big(\int \boldsymbol{f} \times \boldsymbol{u}^L \mathrm{d}z \Big)_\alpha$$
$$+ \partial_\alpha \int \tilde{\pi} \,\mathrm{d}z + \left(\iint \frac{\partial \Omega}{\partial d} \mathcal{N} \mathrm{d}\boldsymbol{k} \; - [\tilde{\pi}]_{-d} \right) \partial_\alpha d = \int u^\circ_\alpha \mathrm{d}z + \iint k_\alpha \mathcal{N}^\circ \,\mathrm{d}\boldsymbol{k}. \tag{3.7}$$

The result

$$\int \mathsf{p}_\alpha u^L_\beta \,\mathrm{d}z = \iint k_\alpha \, \boldsymbol{\mathcal{U}}_\beta \, \mathcal{N} \mathrm{d}\boldsymbol{k}, \tag{3.8}$$

deduced from the definition of the Doppler velocity $\boldsymbol{\mathcal{U}}$ in (2.4) and the definition of pseudomomentum $\mathbf{p}$ in (2.10), produces a further partial cancellation in (3.7):

$$\iint k_\alpha \mathcal{C}_\beta \mathcal{N} \mathrm{d}\boldsymbol{k} - \int \mathsf{p}_\alpha u^L_\beta \,\mathrm{d}z = \iint \mathcal{G} k_\alpha k_\beta \, \mathcal{N} \,\mathrm{d}\boldsymbol{k}, \tag{3.9}$$

where $\mathcal{G}(\boldsymbol{x}, \boldsymbol{k})$ is defined in (2.15). Thus, (3.7) becomes

$$\partial_t \int u^L_\alpha \,\mathrm{d}z + \partial_\beta \left(\int u^L_\alpha u^L_\beta \,\mathrm{d}z + \iint \mathcal{G} \, k_\alpha k_\beta \mathcal{N} \mathrm{d}\boldsymbol{k} \right) + \Big(\int \boldsymbol{f} \times \boldsymbol{u}^L \mathrm{d}z \Big)_\alpha$$
$$+ \partial_\alpha \int \tilde{\pi} \,\mathrm{d}z + \left(\iint \frac{\partial \Omega}{\partial d} \mathcal{N} \mathrm{d}\boldsymbol{k} \; - [\tilde{\pi}]_{-d} \right) \partial_\alpha d = \int u^\circ_\alpha \mathrm{d}z + \iint k_\alpha \mathcal{N}^\circ \,\mathrm{d}\boldsymbol{k}. \tag{3.10}$$

This is momentum conservation in the absence of the Coriolis term, depth variation $\partial_\alpha d$, and of forcing and dissipation on the right-hand side.

Although the pseudomomentum $\mathbf{p}$ appears throughout the manipulations above, remarkable cancellations ensure that $\mathbf{p}$ does not feature in the final form (3.10). This is a manifestation of McIntyre's (1981) 'wave momentum myth': the total momentum density, namely

$$\int \boldsymbol{u}^L \,\mathrm{d}z, \tag{3.11}$$

contains only the Lagrangian mean velocity and the direct effect of the waves in (3.10) is flux of momentum via the radiation stress tensor

$$\iint \mathcal{G} \, k_\alpha k_\beta \mathcal{N} \mathrm{d}\boldsymbol{k}, \tag{3.12}$$

where $\mathcal{G}(\boldsymbol{x}, \boldsymbol{k})$ is defined in (2.15).

As noted by Dewar (1970) we can regard (3.11) as the sum of the Lagrangian mean momentum of the current

$$\int \boldsymbol{u}^L - \mathbf{p} \,\mathrm{d}z \tag{3.13}$$

and the wave pseudomomentum $\int \mathbf{p} \,\mathrm{d}z$ (often termed wave momentum). This is consistent with a geometric interpretation of the Lagrangian mean momentum (Gilbert & Vanneste 2018, 2025). The total momentum (3.11) is the conserved quantity associated with translational symmetry of the system.

In this section, for simplicity, we have focused on the depth-integrated momentum. By forming $\iint (2.1) \boldsymbol{Q}\boldsymbol{k} \,\mathrm{d}\boldsymbol{k}$ and combining with the Craik–Leibovich equation (2.18), it is possible to derive an equation for the total momentum $\boldsymbol{u}^L$ at each z. This equation reduces to (3.10) when integrated with respect to z. It provides an alternative to (2.18) in

https://doi.org/10.1017/jfm.2026.12065 Published online by Cambridge University Press

which wave forcing appears through radiation stresses with vertical as well as horizontal components.

3.3. *Energy conservation*

Following Bretherton & Garrett (1968), we expect that the wave-energy density is

$$\mathcal{E}_w(\boldsymbol{x},\boldsymbol{k}) = \sigma(\boldsymbol{x},\kappa)\,\mathcal{N}(\boldsymbol{x},\boldsymbol{k}), \tag{3.14}$$

where $\sigma(\boldsymbol{x},\kappa)$ is the intrinsic frequency in (2.3). We also expect that the total energy density,

$$E(\boldsymbol{x}) = \int \tfrac{1}{2}|\boldsymbol{u}^L|^2\,\mathrm{d}z + \iint \mathcal{E}_w(\boldsymbol{x},\boldsymbol{k})\,\mathrm{d}\boldsymbol{k}, \tag{3.15}$$

satisfies a physical space conservation law

$$\partial_t E + \boldsymbol{\nabla}_{\boldsymbol{x}}\cdot\boldsymbol{J} = E^\circ. \tag{3.16}$$

The horizontal vector $\boldsymbol{J}(\boldsymbol{x})$ above is the energy flux.

To determine $\boldsymbol{J}$ and E° in (3.16), start with the depth integral of $\boldsymbol{u}^L\cdot$(2.8) and use the vertical boundary conditions (2.12) and (2.13) to find

$$\partial_t \int \tfrac{1}{2}|\boldsymbol{u}^L|^2\,\mathrm{d}z + \boldsymbol{\nabla}_{\boldsymbol{x}}\cdot\int \boldsymbol{u}^L\pi\,\mathrm{d}z = \int \boldsymbol{u}^L\cdot\partial_t\mathbf{p}\,\mathrm{d}z + \int \boldsymbol{u}^L\cdot\boldsymbol{u}^\circ\mathrm{d}z. \tag{3.17}$$

Equation (3.17) is the energy equation for the currents.

Although the wave energy $\mathcal{E}_w$ in (3.14) is related to action density $\mathcal{N}(\boldsymbol{x},\boldsymbol{k})$ by multiplication with the intrinsic frequency $\sigma(\boldsymbol{x},\boldsymbol{k})$, the wave energy conservation law is obtained with $\iint$(3.1)$\Omega\,\mathrm{d}\boldsymbol{k}$, i.e. multiplication of the action conservation equation by the total frequency $\Omega(\boldsymbol{x},\boldsymbol{k}) = \sigma(\boldsymbol{x},\kappa) + \boldsymbol{k}\cdot\boldsymbol{\mathcal{U}}(\boldsymbol{x},\kappa)$. This produces

$$\partial_t\iint \mathcal{E}_w\,\mathrm{d}\boldsymbol{k} + \iint(\boldsymbol{k}\cdot\boldsymbol{\mathcal{U}})\partial_t\mathcal{N}\,\mathrm{d}\boldsymbol{k} + \boldsymbol{\nabla}_{\boldsymbol{x}}\cdot\iint \boldsymbol{\mathcal{C}}\Omega\mathcal{N}\mathrm{d}\boldsymbol{k} = \iint \Omega\mathcal{N}^\circ\mathrm{d}\boldsymbol{k}, \tag{3.18}$$

where $\boldsymbol{\mathcal{C}}$ is the group velocity in (2.14). The key identity

$$\iint(\boldsymbol{k}\cdot\boldsymbol{\mathcal{U}})\,\partial_t\mathcal{N}\,\mathrm{d}\boldsymbol{k} = \int \boldsymbol{u}^L\cdot\iint Q\boldsymbol{k}\,\partial_t\mathcal{N}\,\mathrm{d}\boldsymbol{k}\,\mathrm{d}z = \int \boldsymbol{u}^L\cdot\partial_t\mathbf{p}\,\mathrm{d}z \tag{3.19}$$

then puts (3.18) in the form

$$\partial_t\iint \mathcal{E}_w\,\mathrm{d}\boldsymbol{k} + \int \boldsymbol{u}^L\cdot\partial_t\mathbf{p}\,\mathrm{d}z + \boldsymbol{\nabla}_{\boldsymbol{x}}\cdot\iint \boldsymbol{\mathcal{C}}\Omega\mathcal{N}\mathrm{d}\boldsymbol{k} = \iint \Omega\mathcal{N}^\circ\mathrm{d}\boldsymbol{k}. \tag{3.20}$$

Summing (3.17) and (3.20) eliminates the energy-exchange term

$$\int \boldsymbol{u}^L\cdot\partial_t\mathbf{p}\,\mathrm{d}z \tag{3.21}$$

and produces energy conservation in (3.16) with

$$\boldsymbol{J} = \int \boldsymbol{u}^L\pi\,\mathrm{d}z + \iint \boldsymbol{\mathcal{C}}\Omega\mathcal{N}\,\mathrm{d}\boldsymbol{k}, \tag{3.22}$$

and

$$E^\circ = \iint \Omega\mathcal{N}^\circ\,\mathrm{d}\boldsymbol{k} + \int \boldsymbol{u}^L\cdot\boldsymbol{u}^\circ\,\mathrm{d}z. \tag{3.23}$$

https://doi.org/10.1017/jfm.2026.12065 Published online by Cambridge University Press

The right-hand side of (3.20),

$$\iint \Omega \mathcal{N}^{\circ} \mathrm{d}\boldsymbol{k} = \iint \sigma \mathcal{N}^{\circ} \mathrm{d}\boldsymbol{k} + \iint \boldsymbol{k} \cdot \boldsymbol{\mathcal{U}}\, \mathcal{N}^{\circ} \mathrm{d}\boldsymbol{k}, \tag{3.24}$$

involves a non-obvious contribution of the Doppler shift to E°. We return to this term in § 5.

Using the dispersion relation (2.2), the final term in (3.22) can be split into physically distinct contributions

$$\iint \mathcal{C}\Omega\mathcal{N}\, \mathrm{d}\boldsymbol{k} = \iint \mathcal{C}\mathcal{E}_w\, \mathrm{d}\boldsymbol{k} + \iint \mathcal{G}\boldsymbol{k}\boldsymbol{k} \cdot \boldsymbol{\mathcal{U}}\mathcal{N} \mathrm{d}\boldsymbol{k} + \iint \boldsymbol{\mathcal{U}}\boldsymbol{\mathcal{U}} \cdot \boldsymbol{k}\mathcal{N}\, \mathrm{d}\boldsymbol{k}. \tag{3.25}$$

The first term on the right-hand side of (3.25) is group-velocity transport of the wave energy $\mathcal{E}_w$. The second term is the wave radiation stress (3.12) acting on $\boldsymbol{\mathcal{U}}$. The third term is the momentum flux associated with $\boldsymbol{\mathcal{U}}$ acting on the wave pseudomomentum.

The mean kinetic energy in the conserved energy (3.15) is the LKE $|\boldsymbol{u}^L|^2/2$ rather than the Eulerian kinetic energy (EKE) $|\boldsymbol{u}^E|^2/2$. For the CWCM, this is natural: $\boldsymbol{u}^L$ is the primary dynamical variable and $\boldsymbol{u}^E$ does not appear explicitly. Moreover, the form of the conserved energy is linked to the variational formulation of the CWCM in § 4 via Noether's theorem.

Wagner *et al.* (2021) and Czeschel & Eden (2023) contrast the simplicity of the LKE budget for the (uncoupled) Craik–Leibovich system with the complexity of the EKE budget. The CWCM explains this simplicity by the privileged role of the LKE as one of the two terms in the conserved total energy (3.15). In § 5 we return to the primacy of $|\boldsymbol{u}^L|^2/2$ over $|\boldsymbol{u}^E|^2/2$ in a discussion of wave-forced inertial oscillations. In this basic example the CWCM is forced by prescribing $\mathcal{N}^{\circ}$ in the action transport equation (2.1) and all terms in the energy balance can be calculated explicitly.

3.4. *Circulation and potential vorticity*

Material conservation of circulation and potential vorticity is a property of the Craik–Leibovich equation (2.8), i.e. these laws are independent of the wave-action equation (2.1). We state the results and defer to Andrews & McIntyre (1978) or Holm (1996) for proof.

Introduce the 'absolute Lagrangian mean momentum'

$$\boldsymbol{v}^a = \boldsymbol{h} + \boldsymbol{u}^L - \mathbf{p}, \tag{3.26}$$

where

$$\boldsymbol{h}(\boldsymbol{x}_3) = \tfrac{1}{2}\boldsymbol{f} \times \boldsymbol{x}_3 \tag{3.27}$$

with $\boldsymbol{x}_3 = (\boldsymbol{x}, z)$. A key property of $\boldsymbol{h}$ is that $\boldsymbol{\nabla} \times \boldsymbol{h} = \boldsymbol{f}$. The corresponding absolute vorticity is

$$\boldsymbol{\zeta}^a = \boldsymbol{\nabla} \times \boldsymbol{v}^a = \boldsymbol{f} + \boldsymbol{\nabla} \times (\boldsymbol{u}^L - \mathbf{p}). \tag{3.28}$$

Then conservation of circulation is

$$\frac{\mathrm{d}}{\mathrm{d}t} \oint_{\mathcal{C}} \boldsymbol{v}^a \cdot \mathrm{d}\boldsymbol{\ell} = 0, \tag{3.29}$$

where $\mathcal{C}$ is a material circuit and we assume $\boldsymbol{u}^{\circ} = 0$.

As noted by Andrews & McIntyre (1978), for $\boldsymbol{f} = 0$, conservation of circulation implies that $\boldsymbol{\nabla} \times (\boldsymbol{u}^L - \mathbf{p}) = 0$ for all times if this holds initially. In this irrotational flow regime, $\boldsymbol{u}^L$ is diagnosed from $\mathbf{p}$ as $\boldsymbol{u}^L = \mathbf{p} - \boldsymbol{\nabla}\phi$ for a potential ϕ that is uniquely determined by the Poisson equation $\boldsymbol{\nabla}^2\phi = \boldsymbol{\nabla} \cdot \mathbf{p}$ and the boundary conditions satisfied by $\boldsymbol{u}^L$. The

https://doi.org/10.1017/jfm.2026.12065 Published online by Cambridge University Press

CWCM thus reduces to the action equation (2.1), with $\boldsymbol{\mathcal{U}}(\boldsymbol{x}, \kappa)$ related linearly to $\mathcal{N}(\boldsymbol{x}, \boldsymbol{k})$ via solution of the Poisson equation.

For potential vorticity, suppose that we have a passive scalar $b(\boldsymbol{x}, z, t)$ satisfying wave-averaged material conservation,

$$\partial_t b + \boldsymbol{u}^L \cdot \boldsymbol{\nabla} b = b^\circ. \tag{3.30}$$

Potential vorticity is

$$\Pi = \boldsymbol{\zeta}^a \cdot \boldsymbol{\nabla} b, \tag{3.31}$$

and satisfies

$$\partial_t \Pi + \boldsymbol{u}^L \cdot \boldsymbol{\nabla} \Pi = \boldsymbol{\nabla} \cdot \left(\boldsymbol{u}^\circ \times \boldsymbol{\nabla} b + \boldsymbol{\zeta}^a b^\circ \right). \tag{3.32}$$

4. Variational derivation

The conservation properties of the CWCM can be traced to its variational formulation. We obtain this variational formulation from that of the rotating incompressible Euler equations.

4.1. *Rotating Euler equations*

Variational formulations of fluid models typically involve the flow map, $\boldsymbol{\varphi}$, which sends labels $\boldsymbol{a}$ identifying fluid particles to the time-t positions of the particles, $\boldsymbol{x} = \boldsymbol{\varphi}(\boldsymbol{a}, t)$ (e.g. Salmon 1988). Incompressibility implies that the flow map preserves volume, that is, $|\partial \boldsymbol{\varphi}/\partial \boldsymbol{a}| = \text{const}$. We can take the constant to be 1 without loss of generality. Flow map and velocity field are related via

$$\partial_t \boldsymbol{\varphi}(\boldsymbol{a}, t) = \boldsymbol{u}(\boldsymbol{\varphi}(\boldsymbol{a}, t), t). \tag{4.1}$$

Following Dewar (1970), Bretherton (1971) and Gjaja & Holm (1996) (see also Holm *et al.* (2023)), we make minimal use of labels and flow map by adopting an Eulerian variational formulation. In this formulation – an instance of the Euler–Poincaré framework (Holm *et al.* 1998) – the flow map only appears implicitly through a constrained form of the variations of $\boldsymbol{u}$ first obtained by Newcomb (1962) and Bretherton (1970).

In Appendix B, we show that the rotating, incompressible Euler equations, with a free surface at $z = s(\boldsymbol{x}, t)$, follow from Hamilton's principle $\delta \int \mathcal{L}\, \mathrm{d}t = 0$ applied to the Lagrangian

$$\mathcal{L}[\boldsymbol{u}, s] = \iint \mathrm{d}\boldsymbol{x} \left(\int_{-d}^{s} \left(\frac{1}{2}|\boldsymbol{u}|^2 + \boldsymbol{h} \cdot \boldsymbol{u} \right) \mathrm{d}z - \frac{1}{2} g s^2 \right). \tag{4.2}$$

The Eulerian variations $\delta \boldsymbol{u}$ and δs are induced by variations $\delta \boldsymbol{\varphi}$ of the flow map. Introducing an Eulerian vector field $\boldsymbol{q}(\boldsymbol{x}, t) = (q_1, q_2, q_3)$ by

$$\delta \boldsymbol{\varphi}(\boldsymbol{a}, t) = \boldsymbol{q}(\boldsymbol{\varphi}(\boldsymbol{a}, t), t), \tag{4.3}$$

leads to

$$\delta \boldsymbol{u} = \partial_t \boldsymbol{q} + \boldsymbol{u} \cdot \boldsymbol{\nabla} \boldsymbol{q} - \boldsymbol{q} \cdot \boldsymbol{\nabla} \boldsymbol{u}, \tag{4.4a}$$

$$\delta s = q_3 - q_1 \partial_x s - q_2 \partial_y s, \tag{4.4b}$$

where $\boldsymbol{q}$ satisfies $\boldsymbol{\nabla} \cdot \boldsymbol{q} = 0$ and is otherwise arbitrary (see Appendix B). Incompressibility is enforced by considering only volume-preserving flow maps and hence divergence-free $\boldsymbol{u}$ and $\boldsymbol{q}$. No explicit constraint enforcing $\boldsymbol{\nabla} \cdot \boldsymbol{u} = 0$ is therefore required in (4.2).

https://doi.org/10.1017/jfm.2026.12065 Published online by Cambridge University Press

4.2. *Lagrangian mean framework*

Following the GLM framework, we introduce a wave–mean flow decomposition at the level of the flow map by writing

$$\boldsymbol{\varphi}(\boldsymbol{a}, t) = \bar{\boldsymbol{\varphi}}(\boldsymbol{a}, t) + \boldsymbol{\xi}(\bar{\boldsymbol{\varphi}}(\boldsymbol{a}, t), t), \tag{4.5}$$

where $\bar{\boldsymbol{\varphi}}$ and $\boldsymbol{\xi}$ denote the mean flow and perturbation maps. Below, we introduce a linear-wave ansatz for $\boldsymbol{\xi}$ that captures the wavy displacements resulting from surface gravity waves; $\bar{\boldsymbol{\varphi}}(\boldsymbol{a}, t)$ captures the mean currents.

Differentiating (4.5) with respect to t and using the mean position $\boldsymbol{x}_3 = (\boldsymbol{x}, z) = \bar{\boldsymbol{\varphi}}(\boldsymbol{a}, t)$ as independent variable gives

$$\boldsymbol{u}^{\boldsymbol{\xi}} = \boldsymbol{u}^L + D_t\boldsymbol{\xi}. \tag{4.6}$$

Here, $\boldsymbol{u}^L(\boldsymbol{x}, t)$ defined by

$$\boldsymbol{u}^L(\bar{\boldsymbol{\varphi}}(\boldsymbol{a}), t) = \partial_t\bar{\boldsymbol{\varphi}}(\boldsymbol{a}, t) \tag{4.7}$$

is the Lagrangian mean velocity,

$$D_t = \partial_t + \boldsymbol{u}^L \cdot \boldsymbol{\nabla}, \tag{4.8}$$

and

$$\boldsymbol{u}^{\boldsymbol{\xi}}(\boldsymbol{x}_3, t) = \boldsymbol{u}(\boldsymbol{x}_3 + \boldsymbol{\xi}(\boldsymbol{x}_3, t), t). \tag{4.9}$$

The decomposition (4.5) involves a degree of arbitrariness. We take advantage of this to impose that the mean flow map preserves volume and leaves the free surface flat, that is,

$$|\partial\bar{\boldsymbol{\varphi}}/\partial\boldsymbol{a}| = 1 \quad \text{and} \quad \bar{\varphi}_3(a, b, c = 0) = 0. \tag{4.10}$$

In contrast with standard GLM, the assumptions in (4.10) imply a non-zero average for the perturbation map, $\overline{\boldsymbol{\xi}} \neq 0$ (see Vanneste & Young (2022)). Below in (4.12), however, we use a linear approximation for $\boldsymbol{\xi}$ so that $\overline{\boldsymbol{\xi}}$ vanishes up to neglected terms.

Volume preservation implies that $\boldsymbol{u}^L$ is divergence free, i.e. (2.9). With this, we can rewrite the Lagrangian (4.2) using the mean position $(\boldsymbol{x}, z) = \bar{\boldsymbol{\varphi}}(\boldsymbol{a})$ as an independent variable. This results in

$$\mathcal{L}[\boldsymbol{u}^L, \boldsymbol{\xi}] = \iint \mathrm{d}\boldsymbol{x} \left(\int_{-d}^{0} \frac{1}{2}|\boldsymbol{u}^L + D_t\boldsymbol{\xi}|^2 + \boldsymbol{h}^{\boldsymbol{\xi}} \cdot (\boldsymbol{u}^L + D_t\boldsymbol{\xi})\, \mathrm{d}z - \frac{1}{2}g\zeta^2 \right), \tag{4.11}$$

where $\zeta = \xi_3(\boldsymbol{x}, z = 0)$ and $\boldsymbol{h}^{\boldsymbol{\xi}}(\boldsymbol{x}_3) = \boldsymbol{h}(\boldsymbol{x}_3 + \boldsymbol{\xi}(\boldsymbol{x}_3)) = \boldsymbol{h}(\boldsymbol{x}_3) + (1/2)\boldsymbol{f}\times\boldsymbol{\xi}(\boldsymbol{x}_3)$. (Without the assumption of volume preservation (4.10), (4.11) would contain a Jacobian factor $\tilde{\rho}$, as in the GLM formulation of Andrews & McIntyre (1978).)

4.3. *Averaged Lagrangian*

Up to (4.11) no approximations have been made. We now make a Wentzel–Kramers–Brillouin (WKB) ansatz for $\boldsymbol{\xi}$, assuming a scale separation between rapid phase variations and slow envelope modulations, and Whitham average. Following the prescription of Whitham (1965, 1974), the displacement field $\boldsymbol{\xi}$ is approximated by that of a linear wavetrain,

$$\boldsymbol{\xi} \approx Re\, a(\boldsymbol{x}, t)\hat{\boldsymbol{\xi}}(\boldsymbol{x}, z, \boldsymbol{k})\mathrm{e}^{\mathrm{i}\theta(\boldsymbol{x},t)}, \tag{4.12}$$

https://doi.org/10.1017/jfm.2026.12065 Published online by Cambridge University Press

where $a(\boldsymbol{x}, t)$ is a slowly varying amplitude, $\theta(\boldsymbol{x}, t)$ the phase and $\boldsymbol{k} = (k, l) = \boldsymbol{\nabla}_{\boldsymbol{x}}\theta$. The vertical structure is dictated by

$$\hat{\boldsymbol{\xi}}(\boldsymbol{x}, z, \boldsymbol{k}) = \frac{1}{\kappa \sinh(\kappa d(\boldsymbol{x}))} \begin{pmatrix} \mathrm{i}k \cosh(\kappa(z + d(\boldsymbol{x})) \\ \mathrm{i}l \cosh(\kappa(z + d(\boldsymbol{x})) \\ \kappa \sinh(\kappa(z + d(\boldsymbol{x}))) \end{pmatrix}, \tag{4.13}$$

with $\kappa = |\boldsymbol{k}| = |\boldsymbol{\nabla}_{\boldsymbol{x}}\theta|$. This structure is that obtained for surface waves propagating in a locally uniform current and with locally uniform depth as is usual with the WKB approximation. We also neglect the effect of rotation on the waves, assuming $f \ll \sigma$.

With $\hat{\boldsymbol{\xi}}$ in (4.13), the displacement $\boldsymbol{\xi}(\boldsymbol{x}, t)$ in (4.12) is approximately incompressible and irrotational:

$$\boldsymbol{\nabla} \cdot \boldsymbol{\xi} \approx 0, \qquad \text{and} \qquad \boldsymbol{\nabla} \times \boldsymbol{\xi} \approx 0. \tag{4.14}$$

This approximation is associated with Whitham's variational derivation of the WKB approximation: applying $\boldsymbol{\nabla} = (\boldsymbol{\nabla}_{\boldsymbol{x}}, \partial_z)$ to (4.12) the derivatives act only on the phase $\theta(\boldsymbol{x}, t)$ and on the z-dependence of $\hat{\boldsymbol{\xi}}$. For instance,

$$D_t \boldsymbol{\xi} \approx Re\, a(\boldsymbol{x}, t) \left(\hat{\boldsymbol{\xi}}(\boldsymbol{x}, z, \boldsymbol{k})(-\mathrm{i}\omega + \mathrm{i}\boldsymbol{u}^L \cdot \boldsymbol{k}) + w^L(\boldsymbol{x}, z) \hat{\boldsymbol{\xi}}_z(\boldsymbol{x}, z, \boldsymbol{k}) \right) \mathrm{e}^{\mathrm{i}\theta(\boldsymbol{x}, t)}. \tag{4.15}$$

We further neglect the term involving $w^L \hat{\boldsymbol{\xi}}_z$ in (4.15) on the grounds that $w^L \ll u^L, v^L$.

Introducing (4.12) into the Lagrangian (4.11) and averaging over the phase θ leads to the averaged Lagrangian

$$\overline{\mathcal{L}}[\boldsymbol{u}^L, \theta, a] = \iint \mathrm{d}\boldsymbol{x} \left(\int_{-d}^{0} \left(\frac{1}{2}|\boldsymbol{u}^L|^2 + \boldsymbol{h}(\boldsymbol{x}) \cdot \boldsymbol{u}^L \right) \mathrm{d}z + \frac{1}{4} \left(\int_{-d}^{0} \frac{\cosh(2\kappa(z + d))(\omega - \boldsymbol{k} \cdot \boldsymbol{u}^L)^2}{\sinh^2(\kappa d)} \, \mathrm{d}z - g \right) |a|^2 \right), \tag{4.16}$$

where $\omega = -\partial_t \theta$ and we neglect the wave contributions to the Coriolis term.

Using the definition of $Q(\boldsymbol{x}, z, \kappa)$ in (2.5), we rewrite the second z-integral in (4.16) as

$$\int_{-d}^{0} \frac{\cosh(2\kappa(z + d))(\omega - \boldsymbol{k} \cdot \boldsymbol{u}^L)^2}{\sinh^2(\kappa d)} \, \mathrm{d}z = \frac{1}{\kappa \tanh(\kappa d)} \int_{-d}^{0} (\omega - \boldsymbol{k} \cdot \boldsymbol{u}^L)^2 Q(\boldsymbol{x}, z, \kappa) \, \mathrm{d}z. \tag{4.17}$$

Justified by the smallness of the Doppler shift against the wave frequency, we make the approximation

$$\int_{-d}^{0} (\omega - \boldsymbol{k} \cdot \boldsymbol{u}^L)^2 Q \, \mathrm{d}z = \omega^2 - 2\omega \boldsymbol{k} \cdot \int_{-d}^{0} \boldsymbol{u}^L Q \, \mathrm{d}z + \int_{-d}^{0} (\boldsymbol{k} \cdot \boldsymbol{u}^L)^2 Q \, \mathrm{d}z \tag{4.18a}$$

$$\approx (\omega - \boldsymbol{k} \cdot \boldsymbol{\mathcal{U}})^2, \tag{4.18b}$$

where the Doppler velocity is

$$\boldsymbol{\mathcal{U}} = \int_{-d}^{0} \boldsymbol{u}^L Q \, \mathrm{d}z, \tag{4.19}$$

https://doi.org/10.1017/jfm.2026.12065 Published online by Cambridge University Press

as in (2.4). This manoeuvre simplifies (4.16) to

$$\overline{\mathcal{L}}[\boldsymbol{u}^L, \theta, a] = \iint \mathrm{d}\boldsymbol{x} \left(\int_{-d}^{0} \left(\frac{1}{2}|\boldsymbol{u}^L|^2 + \boldsymbol{h}(\boldsymbol{x}) \cdot \boldsymbol{u}^L \right) \mathrm{d}z + \frac{1}{4} \left(\frac{(\omega - \boldsymbol{k} \cdot \boldsymbol{\mathcal{U}})^2}{\kappa \tanh(\kappa d)} - g \right) |a|^2 \right). \tag{4.20}$$

The approximation in (4.18) is not necessary: one can proceed from the Lagrangian in (4.16). The resulting model has a more complicated dispersion relation than (2.2), and a more complicated expression for the pseudomomentum than (2.10). Alternatively, one obtains a superficially simpler model by boldly dropping the final term in (4.18*a*). But this is one step too many: we prefer the dispersion relation (2.2) with a physically intuitive Doppler shift that preserves Galilean invariance.

The Lagrangian (4.20) is the surface-wave analogue of the Lagrangian obtained by Bretherton (1971), Gjaja & Holm (1996) and Salmon (2016) for acoustic and gravity waves. Hamilton's principle can be applied using variations $\delta\boldsymbol{u}^L$ similar to (4.4*a*), δa and $\delta\theta$. This leads to the Craik–Leibovich system and to equations governing the phase $\theta(\boldsymbol{x}, t)$ and amplitude $a(\boldsymbol{x}, t)$ of a single wavetrain. We do not detail these equations here. Instead, we follow Dewar (1970) to relax the assumption of a single wavetrain and consider a spectrum of linear waves.

4.4. *Variational form of the CWCM*

A spectrum of waves can be regarded as a superposition of independent wavetrains indexed by a two-dimensional (continuous) variable, $\boldsymbol{\alpha}$ say (see Dewar's (1970) discussion of the 'weak turbulence' assumption). Phase $\theta(\boldsymbol{x}, \boldsymbol{\alpha}, t)$ and amplitude $a(\boldsymbol{x}, \boldsymbol{\alpha}, t)$ then depend on $\boldsymbol{\alpha}$, and the Lagrangian (4.20) acquires an additional integration over $\boldsymbol{\alpha}$ to become

$$\overline{\mathcal{L}}[\boldsymbol{u}^L, \theta, a] = \iint \mathrm{d}\boldsymbol{x} \left(\int_{-d}^{0} \left(\frac{1}{2}|\boldsymbol{u}^L|^2 + \boldsymbol{h}(\boldsymbol{x}) \cdot \boldsymbol{u}^L \right) \mathrm{d}z + \frac{1}{4} \iint \left(\frac{(\omega - \boldsymbol{k} \cdot \boldsymbol{\mathcal{U}})^2}{\kappa \tanh(\kappa d)} - g \right) |a|^2 \, \mathrm{d}\boldsymbol{\alpha} \right). \tag{4.21}$$

The representation using $(\boldsymbol{x}, \boldsymbol{\alpha})$ as independent variables and (θ, a) as dependent variables is inconvenient. It is preferable to use instead $(\boldsymbol{x}, \boldsymbol{k})$ as independent variables and $(\omega, \mathcal{N})$ as dependent variables, where

$$\mathcal{N} = \frac{\sigma |a|^2}{2\kappa \tanh(\kappa d)} \left| \frac{\partial \boldsymbol{k}}{\partial \boldsymbol{\alpha}} \right|^{-1}. \tag{4.22}$$

This specific choice ensures that $\mathcal{N}$ is dual to the frequency ω in the sense that $\mathcal{N} = \delta\overline{\mathcal{L}}/\delta\omega$ (see Appendix C). This identifies $\mathcal{N}$ as the wave-action density in $(\boldsymbol{x}, \boldsymbol{k})$-space (Dewar 1970). Making the change of variables in (4.20) puts the averaged Lagrangian in its final form

$$\mathcal{L}_{CWC}[\boldsymbol{u}^L, \mathcal{N}, \omega] = \iint \mathrm{d}\boldsymbol{x} \left(\int_{-d}^{0} \left(\frac{1}{2}|\boldsymbol{u}^L|^2 + \boldsymbol{h}(\boldsymbol{x}) \cdot \boldsymbol{u}^L \right) \mathrm{d}z + \frac{1}{2} \iint (\sigma^{-1}(\omega - \boldsymbol{k} \cdot \boldsymbol{\mathcal{U}})^2 - \sigma)\mathcal{N} \, \mathrm{d}\boldsymbol{k} \right). \tag{4.23}$$

The Lagrangian $\mathcal{L}_{CWC}$ is the Lagrangian of the CWCM. The term on the second line is a standard Whitham-averaged Lagrangian governing wave dynamics. Because of its

https://doi.org/10.1017/jfm.2026.12065 Published online by Cambridge University Press

dependence on the current variable $\boldsymbol{u}^L$ via $\boldsymbol{\mathcal{U}}$, this term contributes to the dynamics of both waves and currents. This is key to consistency of the CWCM.

Hamilton's principle can now be applied to (4.23). The variations are

$$\delta \boldsymbol{u}^L = \partial_t \boldsymbol{q} + \boldsymbol{u}^L \cdot \boldsymbol{\nabla} \boldsymbol{q} - \boldsymbol{q} \cdot \boldsymbol{\nabla} \boldsymbol{u}^L, \tag{4.24}$$

with $\boldsymbol{q}$ satisfying $\boldsymbol{\nabla} \cdot \boldsymbol{q} = 0$ but otherwise arbitrary (in analogy with (4.4*a*)), $\delta \mathcal{N}$ and

$$\delta \omega = \partial_t r + \boldsymbol{\nabla}_{\boldsymbol{x}} r \cdot \boldsymbol{\nabla}_{\boldsymbol{k}} \omega - \boldsymbol{\nabla}_{\boldsymbol{k}} r \cdot \boldsymbol{\nabla}_{\boldsymbol{x}} \omega \tag{4.25}$$

with r arbitrary. This leads to the Craik–Leibovich equation in the form (2.16), dispersion relation (2.2) and action transport equation (2.1). Details are given in Appendix C. The form (4.25) of the variation of ω, reminiscent of (4.24), emerges when changing variables from the mixed Eulerian–Lagrangian $\theta(\boldsymbol{x}, \boldsymbol{\alpha})$ to the Eulerian $\omega(\boldsymbol{x}, \boldsymbol{k})$ (see Dewar (1970) and Appendix D).

5. Hasselmann's problem

Hasselmann (1970) showed that the rectified effect of surface waves is to drive inertial oscillations through 'a vertical shear stress induced by the rotation of the earth'; see also Ursell & Deacon (1950). To exhibit this nonlinear interaction between surface waves and inertial oscillations, we consider a flat-bottom ($\boldsymbol{\nabla}_{\boldsymbol{x}} d = 0$), initially motionless ocean with no waves and no currents:

$$\mathcal{N}(\boldsymbol{x}, \boldsymbol{k}) = \boldsymbol{u}^L(\boldsymbol{x}, z) = 0 \qquad \text{at } t = 0. \tag{5.1}$$

Currents and waves are jointly forced by suddenly switching on horizontally uniform wind forcing. This $t > 0$ forcing is modelled with

$$\mathcal{N}^\circ = \alpha(\mathcal{N}_\star(\boldsymbol{k}) - \mathcal{N}(\boldsymbol{x}, \boldsymbol{k})) \tag{5.2}$$

on the right-hand side of the action transport equation (2.1). In (5.2) $\mathcal{N}_\star(\boldsymbol{k})$ is an equilibrium wave spectrum with pseudomomentum

$$\mathsf{p}_\star(z) = \iint Q(z, \kappa) \mathcal{N}_\star(\boldsymbol{k}) \boldsymbol{k} \, \mathrm{d}\boldsymbol{k} \tag{5.3a}$$

$$= \mathsf{p}_\star(z) \hat{\boldsymbol{x}}. \tag{5.3b}$$

The parameter α in (5.2) controls the rate at which the action spectrum adjusts to the equilibrium spectrum $\mathcal{N}_\star$. In Hasselmann's idealisation, $\mathcal{N}_\star(\boldsymbol{k})$ and $\Omega = \sigma(\kappa) + \boldsymbol{\mathcal{U}}(\kappa) \cdot \boldsymbol{k}$ do not depend on the horizontal coordinates $\boldsymbol{x} = (x, y)$. Thus, there is a horizontally uniform solution of the action (2.1):

$$\mathcal{N}(\boldsymbol{k}, t) = (1 - \mathrm{e}^{-\alpha t}) \mathcal{N}_\star(\boldsymbol{k}). \tag{5.4}$$

The time-varying pseudomomentum is

$$\mathbf{p}(z, t) = (1 - \mathrm{e}^{-\alpha t}) \mathsf{p}_\star(z) \hat{\boldsymbol{x}}. \tag{5.5}$$

Making the traditional approximation that $\boldsymbol{f} = f \hat{\boldsymbol{z}}$ and assuming a solution with the form $\boldsymbol{u}^L = (u^L(z), v^L(z), 0)$, we have

$$\boldsymbol{\nabla} \times (\boldsymbol{u}^L - \mathbf{p}) \times \boldsymbol{u}^L = -\boldsymbol{u}^L \cdot \partial_z (\boldsymbol{u}^L - \mathbf{p}) \, \hat{\boldsymbol{z}}. \tag{5.6}$$

This vertical force is balanced by the vertical pressure gradient.

https://doi.org/10.1017/jfm.2026.12065 Published online by Cambridge University Press

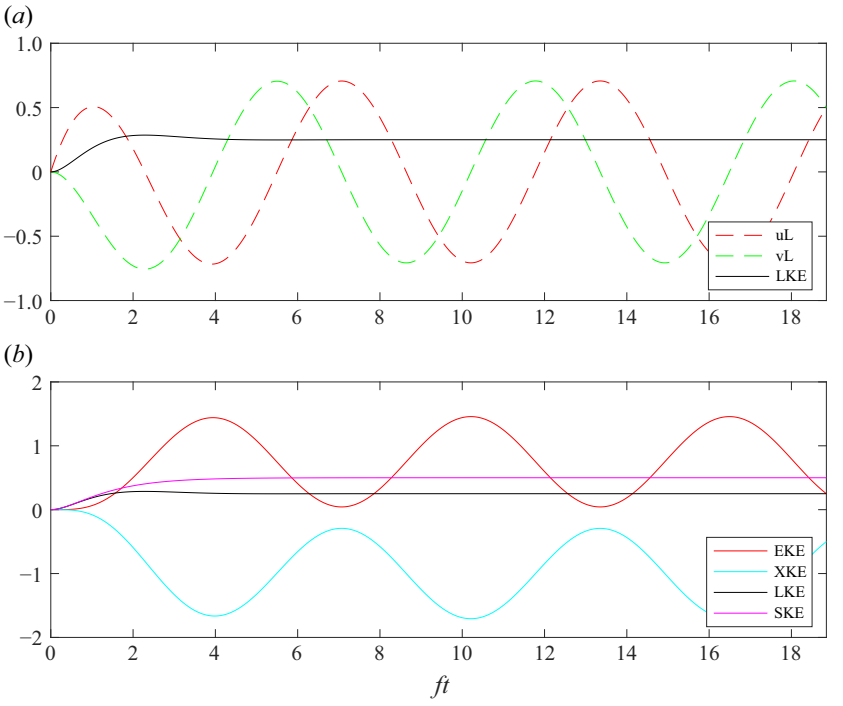


Figure 2. Solution of the Hasselmann problem with $\alpha = f$. (*a*) The dashed sinusoids uL and vL are the scaled Lagrangian velocities $u^L(z,t)/\mathsf{p}_\star(z)$ and $v^L(z,t)/\mathsf{p}_\star(z)$, and LKE $= |\boldsymbol{u}^L|^2/2\mathsf{p}_\star^2$ is the corresponding scaled LKE. (*b*) The four kinetic energy densities defined in (5.12), all scaled with $\mathsf{p}_\star(z)^2$. In this illustration $\alpha/f = 1$.

With $\boldsymbol{u}^\circ = 0$, the horizontal components of $\boldsymbol{u}^L$ evolve according to

$$\partial_t \boldsymbol{u}^L + f\hat{\boldsymbol{z}}\times\boldsymbol{u}^L = \partial_t \boldsymbol{\mathsf{p}} \tag{5.7a}$$

$$= \alpha \mathrm{e}^{-\alpha t}\mathsf{p}_\star \hat{\boldsymbol{x}}. \tag{5.7b}$$

The right-hand side of (5.7*a*) is the inviscid forcing of currents resulting from the 'growth of swell' (Wagner *et al.* 2021).

The solution of (5.7*b*), shown in figure 2(*a*), is

$$u^L + \mathrm{i}v^L = \frac{\alpha \mathsf{p}_\star}{\alpha - \mathrm{i}f}(\mathrm{e}^{-\mathrm{i}ft} - \mathrm{e}^{-\alpha t}) \tag{5.8a}$$

$$\sim \frac{\alpha \mathsf{p}_\star \mathrm{e}^{-\mathrm{i}ft}}{\alpha - \mathrm{i}f} \quad \text{as } t \to \infty. \tag{5.8b}$$

The long-time LKE of the residual inertial oscillation is therefore

$$\frac{1}{2}|\boldsymbol{u}^L|^2 = \frac{1}{2}\frac{\alpha^2 \mathsf{p}_\star^2}{\alpha^2 + f^2}. \tag{5.9}$$

The total work done by the wind in establishing the long-time solution is the sum of the wave energy and the energy in the residual inertial oscillation (5.9):

$$E_w + E_{io} = \iint \sigma(\kappa)\mathcal{N}_\star(\boldsymbol{k})\,\mathrm{d}\boldsymbol{k} + \frac{1}{2}\int_{-d}^{0} \frac{\alpha^2 \mathsf{p}_\star^2(z)}{\alpha^2 + f^2}\,\mathrm{d}z. \tag{5.10}$$

In terms of wave steepness ϵ, E_w is order ϵ^2 while E_{io} of order ϵ^4.

https://doi.org/10.1017/jfm.2026.12065 Published online by Cambridge University Press

Equation (5.10) shows that in Hasselmann's scenario the excitation of inertial waves does not deplete wave energy but is instead achieved through an increase of the wind work. The energy balance (3.16) is consistent with this conclusion: combining the expression for energy production in (3.23) with $\Omega = \sigma + \boldsymbol{k}\cdot\boldsymbol{\mathcal{U}}$, (3.16) reduces to

$$\partial_t E = \underbrace{\iint \sigma \mathcal{N}^{\circ} \mathrm{d}\boldsymbol{k}}_{\partial_t E_w} + \underbrace{\iint \boldsymbol{k}\cdot\boldsymbol{\mathcal{U}} \mathcal{N}^{\circ} \mathrm{d}\boldsymbol{k}}_{\partial_t E_{io}} . \tag{5.11}$$

The final term in (5.11) is the production by wind of near-inertial energy, E_{io} in (5.10).

The assumption of horizontal uniformity ensures that $\boldsymbol{\nabla}_{\boldsymbol{k}}\,\Omega\cdot\boldsymbol{\nabla}_{\boldsymbol{x}}\mathcal{N} - \boldsymbol{\nabla}_{\boldsymbol{x}}\,\Omega\cdot\boldsymbol{\nabla}_{\boldsymbol{k}}\,\mathcal{N} = 0$ in (2.1), i.e. the inertial current in (5.9) has no effect on $\mathcal{N}(\boldsymbol{x},\boldsymbol{k},t)$. It is possible, however, that the inertial oscillation is linearly unstable, and saturation of this instability might lead to turbulent currents and modification of $\mathcal{N}$ by currents. This possibility is strongly indicated by the numerical solutions of Wagner *et al.* (2021) in which the pseudomomentum $\mathsf{p}(z,t)$ is prescribed. In fact, prescription of $\mathsf{p}(z,t)$ is recovered as the special case $\alpha\to\infty$ of the relaxation-to-$\mathcal{N}_\star$ model in (5.2).

The 'LKE density' is partitioned by the decomposition $\boldsymbol{u}^L = \boldsymbol{u}^E + \boldsymbol{u}^S$ (with $\boldsymbol{u}^S \approx \mathsf{p}$) into

$$\underbrace{\tfrac{1}{2}|\boldsymbol{u}^L|^2}_{\text{LKE}} = \underbrace{\tfrac{1}{2}|\boldsymbol{u}^E|^2}_{\text{EKE}} + \underbrace{\boldsymbol{u}^S\cdot\boldsymbol{u}^E}_{\text{XKE}} + \underbrace{\tfrac{1}{2}|\boldsymbol{u}^S|^2}_{\text{SKE}} . \tag{5.12}$$

In (5.12), the LKE density produces E_{io} when integrated in z, XKE is the kinetic energy in the 'cross-term' $\boldsymbol{u}^E\cdot\boldsymbol{u}^S$ and SKE is the Stokes kinetic energy. Figure 2(*b*) shows these four kinetic energy densities in the $\alpha/f = 1$ solution. LKE is smaller in magnitude than the three terms on the right-hand side of (5.12) and, unlike EKE and XKE, has simple monotonic evolution. The same conclusions are drawn by Czeschel & Eden (2023).

In the long-time limit $\mathrm{e}^{-\alpha t}\to 0$, the decomposition in (5.12) is

$$\underbrace{\tfrac{1}{2}\frac{\alpha^2\mathsf{p}_\star^2}{\alpha^2+f^2}}_{\text{LKE}} = \underbrace{\tfrac{1}{2}|\boldsymbol{u}^E|^2 + \boldsymbol{u}^E\cdot\boldsymbol{u}^S}_{\text{EKE + XKE}} + \underbrace{\tfrac{1}{2}\mathsf{p}_\star^2}_{\text{SKE}} . \tag{5.13}$$

EKE and XKE both oscillate at the inertial frequency, but their sum is steady and negative:

$$\text{EKE + XKE} = -\tfrac{1}{2}\frac{f^2\mathsf{p}_\star^2}{\alpha^2+f^2} \leqslant 0. \tag{5.14}$$

In the long-time limit XKE is negative and greater in magnitude than EKE for all values of α/f.

When viewed in terms of the monotonically increasing LKE in figure 2, the energetics of Hasselmann's problem is straightforward: wave forcing via $\mathsf{p}(z,t)$ is steadily increasing the LKE of the currents. But when viewed in terms of EKE and XKE this simple result is obscured and the problem seems complicated and confusing. This Lagrangian simplicity is because $|\boldsymbol{u}^L|^2/2$ is the current kinetic energy that participates in the complete and consistent energy conservation law in (3.15) and (3.16).

The Doppler velocity takes the form

$$\begin{aligned}\mathcal{U} + \mathrm{i}\mathcal{V} &= \int_{-d}^{0} Q(\kappa,z)(u^L + \mathrm{i}v^L)\,\mathrm{d}z \\ &= \frac{\alpha}{\alpha - \mathrm{i}f}(\mathrm{e}^{-\mathrm{i}ft} - \mathrm{e}^{-\alpha t}) \int \Lambda(\kappa,\kappa')\mathcal{N}_\star(\boldsymbol{k}')\boldsymbol{k}'\,\mathrm{d}\boldsymbol{k}',\end{aligned} \tag{5.15}$$

https://doi.org/10.1017/jfm.2026.12065 Published online by Cambridge University Press

where

$$\Lambda(\kappa,\kappa') = \int_{-d}^{0} Q(\kappa,z)\,Q(\kappa',z)\,\mathrm{d}z = \frac{2\kappa\kappa'}{\kappa+\kappa'}\,\frac{\kappa\coth(2\kappa' d)-\kappa'\coth(2\kappa d)}{\kappa-\kappa'}. \tag{5.16}$$

The general argument of § 3.3 shows that introducing (5.15) into the right-hand side of (5.11) recovers $\partial_t E_{io}$.

6. Discussion

The CWCM, the model of two-way coupling between surface waves and ocean currents introduced in § 2, is perhaps the simplest that conserves momentum and energy. This simplicity is achieved in part by adopting a wave–mean separation that differs from standard GLM to ensure (i) that the mean current is exactly divergence free, and (ii) that the mean free surface is flat. Property (ii) amounts to restricting mean configurations to those that minimise gravitational potential energy. Such a restriction is standard in the treatment of dynamical systems under a strong constraining potential (e.g. Takens 1980). It has the benefit of filtering surface waves from the mean equations. Property (ii) does not preclude capturing mean deformations in the free-surface elevation: in principle, these mean deformations are represented through non-zero mean perturbations, $\overline{\boldsymbol{\xi}} \neq 0$. Our formulation, however, ignores these by following Whitham and using the linear approximation (4.13) for $\boldsymbol{\xi}$.

The simplicity of the CWCM also stems from the variational approach used for its derivation. Compared with formal asymptotic expansions carried out at the level of the dynamical equations, the variational approach has the advantage of preservation of symmetry-related conservation and ease of implementation. (Exploratory calculations indicate that systematic asymptotics to fourth order in wave steepness, as required to capture terms such as $|\boldsymbol{u}^S|^2/2$ in the energy equation, is exceedingly complicated.) Against this, an inconvenience is the difficulty in ascertaining the asymptotic accuracy of the variational model. But for a problem as complex as the two-way interactions between surface gravity waves and currents, involving multiple small parameters and regimes of physical interest, we believe that the variational formulation has overwhelming advantages.

The CWCM in § 2, with conservation laws on display in § 3, follows from the application of Hamilton's principle to the Lagrangian $\mathcal{L}_{CWC}$ in (4.23). The primary approximation used in the construction $\mathcal{L}_{CWC}$ is Whitham's linear-wave approximation in (4.12) and (4.13). We then make a few secondary approximations, such as simplification of the Doppler shift as in (4.18). These secondary approximations can be avoided at the expense of a more complicated model. For example, retaining $w^L\hat{\boldsymbol{\xi}}_z$ in (4.15) results in a three-dimensional pseudomomentum. Presumably this more complicated model is also a more accurate representation of the two-way interaction between currents and waves.

Controversial issues such as the divergence and vertical component of $\mathbf{p} \approx \boldsymbol{u}^S$ or whether the current kinetic energy involves $\boldsymbol{u}^E$ or $\boldsymbol{u}^L$ do not arise in our formulation. Only the Lagrangian mean velocity $\boldsymbol{u}^L$ and pseudomomentum $\mathbf{p}$ play a dynamical role. The pseudomomentum $\mathbf{p}$ appears as the variational derivative of the wave Lagrangian with respect to $\boldsymbol{u}^L$, a vector directly related to wave action, rather than as an approximation to the general three-dimensional form of Andrews & McIntyre (1978). The primacy of $\boldsymbol{u}^L$ and $\mathbf{p}$ over $\boldsymbol{u}^E$ and $\boldsymbol{u}^S$ is an unavoidable feature of variational formulations of coupled wave–mean models. This aspect of the CWCM will remain if some of the approximations we have made are relaxed.

The CWCM provides a sound basis for revisiting problems that have previously been examined with prescribed $\boldsymbol{u}^S$ or $\mathbf{p}$. The generation of inertial oscillations by a uniform

https://doi.org/10.1017/jfm.2026.12065 Published online by Cambridge University Press

field of surface waves considered in § 5 is the simplest such problem. Because of the assumption of horizontal homogeneity, the dynamics of action is not affected the mean current that is generated. The main benefit of the CWCM is then to provide a consistent picture of the energy exchanges between wind, waves and currents. It will be interesting to consider problems in which currents and wave action vary in the horizontal so that the two-way interactions come into play. These problems include instabilities such as the Craik–Leibovich instability responsible for the formation of Langmuir cells. Stratification effects can be included straightforwardly by treating buoyancy as a passive scalar, as in (3.30), and adding the buoyancy force in the momentum equation.

Applications of the Craik–Leibovich system to realistic ocean conditions often involve turbulence. The exchanges between waves and currents are then complicated by the separation of the currents into mean and turbulent components and the need to parameterise turbulent fluxes (e.g. Suzuki & Fox-Kemper 2016; Czeschel & Eden 2023). Work along these lines should use the CWCM or a similar model that recognises the importance of the LKE $|\boldsymbol{u}^L|^2/2$.

Acknowledgements. We thank O. Bokhove, L. Czeschel and G. Wagner for useful discussions and the anonymous referees for their valuable comments.

Funding. J.V. is supported by the UK Natural Environment Research Council (grant NE/W002876/1). W.R.Y. is supported by the National Science Foundation award 2048583.

Declaration of interests. The authors report no conflict of interest.

Appendix A. The integral involving $\partial_\alpha \Omega$ in (3.3)

The most difficult term in (3.3) is

$$\iint \mathcal{N}\partial_\alpha \Omega \,\mathrm{d}\boldsymbol{k} = \iint \mathcal{N}\partial_\alpha \Big[\sigma(d(\boldsymbol{x}), \boldsymbol{k}) + \int_{-d(\boldsymbol{x})}^{0} Q(d(\boldsymbol{x}), z, \kappa)\boldsymbol{k}\cdot\boldsymbol{u}^L(\boldsymbol{x}, z)\,\mathrm{d}z\Big]\,\mathrm{d}\boldsymbol{k}. \quad \text{(A1)}$$

On the right-hand side of (A1) we have written the Doppler shifted frequency $\Omega(\boldsymbol{x}, \boldsymbol{k})$ expansively and indicated that the $\boldsymbol{x}$-dependence of σ and Q is exclusively through the depth $d(\boldsymbol{x})$. Notice that the derivative ∂_α acts on $d(\boldsymbol{x})$ and also on the separate $\boldsymbol{x}$-dependence of $\boldsymbol{u}^L(\boldsymbol{x}, z)$. We have

$$\iint \mathcal{N}\partial_\alpha \Omega \,\mathrm{d}\boldsymbol{k} = \iint \mathcal{N}\int_{-d}^{0} Q(d, z, \kappa)\boldsymbol{k}\cdot\partial_\alpha \boldsymbol{u}^L \,\mathrm{d}z\,\mathrm{d}\boldsymbol{k} + \iint \mathcal{N}\frac{\partial \Omega}{\partial d}\,\mathrm{d}\boldsymbol{k}\,\partial_\alpha d. \quad \text{(A2)}$$

Most of the complication is in

$$\frac{\partial \Omega}{\partial d} = \frac{\partial \sigma}{\partial d} + \boldsymbol{k}\cdot\int_{-d}^{0}\frac{\partial Q}{\partial d}\boldsymbol{u}^L(\boldsymbol{x}, z)\,\mathrm{d}z + \boldsymbol{k}\cdot[Q\boldsymbol{u}^L]_{-d}. \quad \text{(A3)}$$

Above, $[\,]_{-d}$ indicates evaluation at $z = -d(\boldsymbol{x})$, i.e. $[Q\boldsymbol{u}^L]_{-d} = Q(d, -d, \kappa)\boldsymbol{u}^L(\boldsymbol{x}, -d)$. Switching the order of the z- and $\boldsymbol{k}$-integrals in the first term on the right-hand side of (A2) produces

$$\iint \mathcal{N}\partial_\alpha \Omega \,\mathrm{d}\boldsymbol{k} = \int_{-d}^{0} \mathsf{p}_\beta \partial_\alpha u_\beta^L \,\mathrm{d}z + \iint \mathcal{N}\frac{\partial \Omega}{\partial d}\,\mathrm{d}\boldsymbol{k}\,\partial_\alpha d, \quad \text{(A4)}$$

where we have used the definition of the pseudomomentum in (2.10).

https://doi.org/10.1017/jfm.2026.12065 Published online by Cambridge University Press

There is an interesting alternative expression for $\partial\Omega/\partial d$ in (A3). We first establish a useful identity: ∂_α of the $Q(\boldsymbol{x}, z, \kappa)$ normalisation integral (2.6) produces

$$\int_{-d}^{0} \partial_\alpha Q \, \mathrm{d}z + [Q]_{-d}\partial_\alpha d = 0. \tag{A5}$$

Substituting

$$\partial_\alpha Q = \frac{\partial Q}{\partial d}\,\partial_\alpha d \tag{A6}$$

into (A5) and cancelling $\partial_\alpha d$ produces the identity

$$\int_{-d}^{0} \frac{\partial Q}{\partial d}\mathrm{d}z + [Q]_{-d} = 0. \tag{A7}$$

Using (A7) to eliminate $[Q]_{-d}$ from (A3):

$$\frac{\partial \Omega}{\partial d} = \frac{\partial \sigma}{\partial d} + \boldsymbol{k}\cdot\int_{-d}^{0} \frac{\partial Q}{\partial d}(\boldsymbol{u}^L - [\boldsymbol{u}^L]_{-d})\,\mathrm{d}z. \tag{A8}$$

In the shallow-water limit, with $\boldsymbol{u}^L$ independent of z, only $\partial\sigma/\partial d$ remains.

Appendix B. Variational derivation of the rotating Euler equations

We derive the rotating incompressible Euler equations from Hamilton's principle applied to the Lagrangian (4.2) with constrained variations (4.4). We start by deriving the constrained variations (4.4) and (4.25) following Newcomb (1962), Bretherton (1970) and Dewar (1970).

B.1 *Variations $\delta\boldsymbol{u}$ and δs*

The variations $\delta\boldsymbol{u}(\boldsymbol{x}, t)$ of the velocity field are induced by variations $\delta\boldsymbol{\varphi}(\boldsymbol{a}, t)$ of the flow map. Taking the time derivative of (4.3) gives

$$\begin{aligned}\partial_t\delta\boldsymbol{\varphi}(\boldsymbol{a}, t) &= \partial_t\boldsymbol{q}(\boldsymbol{\varphi}(\boldsymbol{a}, t), t) + \partial_t\boldsymbol{\varphi}(\boldsymbol{a}, t)\cdot\boldsymbol{\nabla}\boldsymbol{q}(\boldsymbol{\varphi}(\boldsymbol{a}, t), t)\\ &= \partial_t\boldsymbol{q}(\boldsymbol{\varphi}(\boldsymbol{a}, t), t) + \boldsymbol{u}(\boldsymbol{\varphi}(\boldsymbol{a}, t), t)\cdot\boldsymbol{\nabla}\boldsymbol{q}(\boldsymbol{\varphi}(\boldsymbol{a}, t), t).\end{aligned} \tag{B1}$$

Another expression for the left-hand side is obtained by taking variations of $\partial_t\boldsymbol{\varphi}(\boldsymbol{a}, t) = \boldsymbol{u}(\boldsymbol{\varphi}(\boldsymbol{a}, t), t)$ and using the equality $\delta\partial_t = \partial_t\delta$ of mixed derivatives to find

$$\begin{aligned}\partial_t\delta\boldsymbol{\varphi}(\boldsymbol{a}, t) &= \delta\boldsymbol{u}(\boldsymbol{\varphi}(\boldsymbol{a}, t), t) + \delta\boldsymbol{\varphi}(\boldsymbol{a}, t)\cdot\boldsymbol{\nabla}\boldsymbol{u}(\boldsymbol{\varphi}(\boldsymbol{a}, t), t)\\ &= \delta\boldsymbol{u}(\boldsymbol{\varphi}(\boldsymbol{a}, t), t) + \boldsymbol{q}(\boldsymbol{\varphi}(\boldsymbol{a}, t), t)\cdot\boldsymbol{\nabla}\boldsymbol{u}(\boldsymbol{\varphi}(\boldsymbol{a}, t), t).\end{aligned} \tag{B2}$$

Equating (B1) and (B2) gives (4.4*a*).

The form (4.4*b*) of δs is obtained by relating free surface elevation and flow map via

$$s(\varphi_1(a, b, 0), \varphi_2(a, b, 0), t) = \varphi_3(a, b, 0, t), \tag{B3}$$

where $\boldsymbol{a} = (a, b, 0)$ parameterises the free surface in label space. Taking variations gives

$$\delta s(\boldsymbol{x}, t) + \delta\varphi_1(a, b, 0, t)\partial_x s(\boldsymbol{x}, t) + \delta\varphi_2(a, b, 0, t)\partial_y s(\boldsymbol{x}, t) = \delta\varphi_3(a, b, 0, t), \tag{B4}$$

that is,

$$\delta s(\boldsymbol{x}, t) + q_1(\boldsymbol{x}, t)\partial_x s(\boldsymbol{x}, t) + q_2(\boldsymbol{x}, t)\partial_y s(\boldsymbol{x}, t) = q_3(\boldsymbol{x}, t), \tag{B5}$$

where $\boldsymbol{x} = (\varphi_1(a, b, 0, t), \varphi_2(a, b, 0, t))$. Rearranging gives (4.4*b*). The assumption of volume preserving flow map implies that $\boldsymbol{\nabla}\cdot\boldsymbol{q} = 0$.

https://doi.org/10.1017/jfm.2026.12065 Published online by Cambridge University Press

B.2 *Hamilton's principle applied to (4.2)*

Hamilton's principle states that

$$\delta \int \mathcal{L}\,\mathrm{d}t = \delta \int \mathrm{d}t \iint \mathrm{d}\boldsymbol{x} \left(\int_{-d}^{s} \boldsymbol{u}^a \cdot \delta \boldsymbol{u}\,\mathrm{d}z + \left(\left[\tfrac{1}{2}|\boldsymbol{u}|^2 + \boldsymbol{h}\cdot\boldsymbol{u} \right]_s - gs \right) \delta s \right) = 0, \quad \text{(B6)}$$

where $\boldsymbol{u}^a = \boldsymbol{u} + \boldsymbol{h}$ and $[\,\cdot\,]_s$ denotes evaluation at $z = s$. We use (4.4*a*) and manipulate the z integral:

$$\begin{aligned} \int_{-d}^{s} \boldsymbol{u}^a \cdot \delta \boldsymbol{u}\,\mathrm{d}z &= \int_{-d}^{s} \boldsymbol{u}^a \cdot (\partial_t \boldsymbol{q} + \boldsymbol{u}\cdot\boldsymbol{\nabla}\boldsymbol{q} - \boldsymbol{q}\cdot\boldsymbol{\nabla}\boldsymbol{u})\,\mathrm{d}z \\ &= \int_{-d}^{s} \Big(\partial_t (\boldsymbol{u}^a \cdot \boldsymbol{q}) + \boldsymbol{\nabla}\cdot(\boldsymbol{u}^a \cdot \boldsymbol{q}\,\boldsymbol{u}) \\ &\qquad - (\partial_t \boldsymbol{u} + \boldsymbol{u}\cdot\boldsymbol{\nabla}\boldsymbol{u}^a + \boldsymbol{\nabla}\boldsymbol{u}\cdot\boldsymbol{u}^a)\cdot\boldsymbol{q} \Big)\,\mathrm{d}z\,. \end{aligned} \quad \text{(B7)}$$

In $\boldsymbol{\nabla}\boldsymbol{u}\cdot\boldsymbol{u}^a$, the contraction is between $\boldsymbol{u}$ and $\boldsymbol{u}^a$, i.e. in coordinates, $(\boldsymbol{\nabla}\boldsymbol{u}\cdot\boldsymbol{u}^a)_i = (\partial_i u_j)u^a_j$. We repeatedly use this convention below. Integrating (B7) with respect to $\boldsymbol{x}$ and using the Reynolds transport theorem gives

$$\begin{aligned} \iint \mathrm{d}\boldsymbol{x} \int_{-d}^{s} \boldsymbol{u}^a \cdot \delta \boldsymbol{u}\,\mathrm{d}z &= \frac{\mathrm{d}}{\mathrm{d}t} \iint \mathrm{d}\boldsymbol{x} \int_{-d}^{s} \boldsymbol{u}^a \cdot \boldsymbol{q}\,\mathrm{d}z \\ &\quad - \iint \mathrm{d}\boldsymbol{x} \int_{-d}^{s} (\partial_t \boldsymbol{u} + \boldsymbol{u}\cdot\boldsymbol{\nabla}\boldsymbol{u}^a + \boldsymbol{\nabla}\boldsymbol{u}\cdot\boldsymbol{u}^a)\cdot\boldsymbol{q} \Big)\,\mathrm{d}z. \end{aligned} \quad \text{(B8)}$$

Here we impose the kinematic boundary condition $\partial_t s + u\partial_x s + v\partial_y s = w$ at $z = s(\boldsymbol{x}, t)$ and the no-normal flow condition $w + \boldsymbol{u}\cdot\boldsymbol{\nabla}_{\boldsymbol{x}} d = 0$ at $z = -d(\boldsymbol{x})$.

The exact time derivative on the first line of (B8) does not contribute to (B6) because $\boldsymbol{q}$ is assumed to vanish at the endpoints of the time integral. The second line makes a contribution that vanishes for all divergence-free $\boldsymbol{q}$, as required, provided that

$$\partial_t \boldsymbol{u} + \boldsymbol{u}\cdot\boldsymbol{\nabla}\boldsymbol{u}^a + \boldsymbol{\nabla}\boldsymbol{u}\cdot\boldsymbol{u}^a = -\boldsymbol{\nabla}\pi \quad \text{(B9)}$$

for some scalar field π. (This follows from Helmholtz decomposing $\partial_t \boldsymbol{u} + \boldsymbol{u}\cdot\boldsymbol{\nabla}\boldsymbol{u}^a + \boldsymbol{\nabla}\boldsymbol{u}\cdot\boldsymbol{u}^a$ and observing that the vanishing of (B8) implies that the rotational part is zero.) Using vector calculus identities, (B9) can be rewritten as

$$\partial_t \boldsymbol{u} + (\boldsymbol{\nabla}\times\boldsymbol{u}^a)\times\boldsymbol{u} = -\boldsymbol{\nabla}(\pi + \boldsymbol{u}^a\cdot\boldsymbol{u}), \quad \text{(B10)}$$

then as

$$\partial_t \boldsymbol{u} + \boldsymbol{u}\cdot\boldsymbol{\nabla}\boldsymbol{u} + \boldsymbol{f}\times\boldsymbol{u} = -\boldsymbol{\nabla} p, \quad \text{(B11)}$$

where $p = \pi + \frac{1}{2}|\boldsymbol{u}|^2 + \boldsymbol{h}\cdot\boldsymbol{u}$. This is the familiar form of the rotating Euler equations.

With (B9) and using $\boldsymbol{\nabla}\cdot\boldsymbol{q} = 0$, the second line in (B8) becomes

$$\iint \mathrm{d}\boldsymbol{x} \int_{-d}^{s} \boldsymbol{\nabla}\cdot(\pi\boldsymbol{q})\,\mathrm{d}z = \iint \mathrm{d}\boldsymbol{x}\,[\pi\,\boldsymbol{n}\cdot\boldsymbol{q}]_s = \iint \mathrm{d}\boldsymbol{x}\;[\pi]_s\,\delta s, \quad \text{(B12)}$$

where $\boldsymbol{n} = (-\boldsymbol{\nabla}_{\boldsymbol{x}} s, 1)$ and we use the form (4.4b) of δs and that $\boldsymbol{q}$ is tangent to the bottom boundary. This reduces Hamilton's principle (B6) to surface terms:

$$\delta \int \mathcal{L}\,\mathrm{d}t = \delta \int \mathrm{d}t \iint \mathrm{d}\boldsymbol{x} \left(\left[\pi + \tfrac{1}{2}|\boldsymbol{u}|^2 + \boldsymbol{h}\cdot\boldsymbol{u} \right]_s - gs \right) \delta s. \quad \text{(B13)}$$

https://doi.org/10.1017/jfm.2026.12065 Published online by Cambridge University Press

Imposing that these vanish leads to the dynamic boundary condition

$$p = gs. \tag{B14}$$

Appendix C. Variational derivation of the CWCM

We derive the coupled model governed by (2.1)–(2.12) from Hamilton's principle applied to the averaged Lagrangian $\mathcal{L}_{CWC}$ in (4.20) with variations (4.24) and (4.25). The variations $\delta\mathcal{N}$ are unconstrained, hence Hamilton's principle implies that

$$\frac{\delta\overline{\mathcal{L}}}{\delta\mathcal{N}} = \sigma^{-1}(\omega - \boldsymbol{k}\cdot\boldsymbol{\mathcal{U}})^2 - \sigma = 0. \tag{C1}$$

The dispersion relation $\omega = \sigma + \boldsymbol{k}\cdot\boldsymbol{\mathcal{U}} = \Omega(\boldsymbol{x},\boldsymbol{k})$ follows. Using this, we compute

$$\begin{aligned}\frac{\delta\overline{\mathcal{L}}}{\delta\boldsymbol{u}^L} &= \boldsymbol{u}^L + \boldsymbol{h} - \iint Q(\boldsymbol{x},z,\kappa)\mathcal{N}(\boldsymbol{x},\boldsymbol{k})\boldsymbol{k}\,\mathrm{d}\boldsymbol{k}\\ &= \boldsymbol{u}^L + \boldsymbol{h} - \mathsf{p} = \boldsymbol{v}^a\end{aligned} \tag{C2}$$

and

$$\frac{\delta\overline{\mathcal{L}}}{\delta\omega} = \mathcal{N}. \tag{C3}$$

With these results, Hamilton's principle reduces to

$$\delta\int\mathcal{L}\,\mathrm{d}t = \delta\int\mathrm{d}t\iint\mathrm{d}\boldsymbol{x}\left(\int_{-d}^{0}\boldsymbol{v}^a\cdot\delta\boldsymbol{u}^L\,\mathrm{d}z + \iint\mathcal{N}\delta\omega\,\mathrm{d}\boldsymbol{k}\right) = 0. \tag{C4}$$

The variations $\delta\boldsymbol{u}^L$ and $\delta\omega$ are independent and can be treated separately.

For $\delta\boldsymbol{u}^L$, (4.24) gives

$$\begin{aligned}\iint\mathrm{d}\boldsymbol{x}\int_{-d}^{0}\boldsymbol{v}^a\cdot\delta\boldsymbol{u}^L\,\mathrm{d}z &= \iint\mathrm{d}\boldsymbol{x}\int_{-d}^{0}\boldsymbol{v}^a\cdot(\partial_t\boldsymbol{q} + \boldsymbol{u}^L\cdot\nabla\boldsymbol{q} - \boldsymbol{q}\cdot\nabla\boldsymbol{u}^L)\,\mathrm{d}z\\ &= \iint\mathrm{d}\boldsymbol{x}\int_{-d}^{0}\partial_t(\boldsymbol{v}^a\cdot\boldsymbol{q}) + \nabla\cdot(\boldsymbol{v}^a\cdot\boldsymbol{q}\,\boldsymbol{u}^L)\\ &\qquad - (\partial_t\boldsymbol{v}^a + \boldsymbol{u}^L\cdot\nabla\boldsymbol{v}^a + \nabla\boldsymbol{u}^L\cdot\boldsymbol{v}^a)\cdot\boldsymbol{q}\,\mathrm{d}z.\end{aligned} \tag{C5}$$

The terms on the first line make no contributions to (C4), bar boundary terms that vanish provided that the boundary conditions (2.12) and (2.13) hold. The terms on the second line vanish for all divergence-free $\boldsymbol{q}$ provided that

$$\partial_t\boldsymbol{v}^a + \boldsymbol{u}^L\cdot\nabla\boldsymbol{v}^a + \nabla\boldsymbol{u}^L\cdot\boldsymbol{v}^a = -\nabla\hat{\pi} \tag{C6}$$

for some scalar $\hat{\pi}$. We recognise (C6) as version (2.16) of the Craik–Leibovich equation in vector form and with $\boldsymbol{u}^\circ = 0$.

For $\delta\omega$, (4.25) gives

$$\begin{aligned}\iint\mathrm{d}\boldsymbol{x}\iint\mathcal{N}\delta\omega\,\mathrm{d}\boldsymbol{k} &= \iint\mathrm{d}\boldsymbol{x}\iint\mathcal{N}(\partial_t r + \nabla_{\boldsymbol{x}}r\cdot\nabla_{\boldsymbol{k}}\omega - \nabla_{\boldsymbol{k}}r\cdot\nabla_{\boldsymbol{x}}\omega)\,\mathrm{d}\boldsymbol{k}\\ &= \iint\mathrm{d}\boldsymbol{x}\iint\Big(\partial_t(\mathcal{N}r) + \nabla_{\boldsymbol{x}}\cdot(\mathcal{N}r\nabla_{\boldsymbol{k}}\omega) - \nabla_{\boldsymbol{k}}\cdot(\mathcal{N}r\nabla_{\boldsymbol{x}}\omega)\\ &\qquad - (\partial_t\mathcal{N} + \nabla_{\boldsymbol{k}}\omega\cdot\nabla_{\boldsymbol{x}}\mathcal{N} - \nabla_{\boldsymbol{x}}\omega\cdot\nabla_{\boldsymbol{k}}\mathcal{N})r\Big)\,\mathrm{d}\boldsymbol{k}.\end{aligned} \tag{C7}$$

https://doi.org/10.1017/jfm.2026.12065 Published online by Cambridge University Press

Again, the terms in the first line are total derivatives and make no contribution to (C4). The vanishing of the remaining terms for arbitrary r implies the wave-action transport equation (2.1) with $\mathcal{N}^\circ = 0$.

Appendix D. Constrained variation $\delta\boldsymbol{\omega}$

The variation $\delta\omega$ in (4.25) arises from unconstrained the variation $\delta\theta(\boldsymbol{x}, \boldsymbol{\alpha}, t)$ via the change of dependent and independent variables

$$(\boldsymbol{x}, \boldsymbol{\alpha}, \theta(\boldsymbol{x}, \boldsymbol{\alpha}, t)) \mapsto (\boldsymbol{x}, \boldsymbol{k}, \omega(\boldsymbol{x}, \boldsymbol{k}, t)) \tag{D1}$$

with

$$\boldsymbol{k} = \boldsymbol{K}(\boldsymbol{x}, \boldsymbol{\alpha}, t) \overset{\text{def}}{=} \boldsymbol{\nabla}_{\boldsymbol{x}}\theta(\boldsymbol{x}, \boldsymbol{\alpha}, t) \quad \text{and} \quad \omega(\boldsymbol{x}, \boldsymbol{K}(\boldsymbol{x}, \boldsymbol{\alpha}, t), t) = -\partial_t\theta(\boldsymbol{x}, \boldsymbol{\alpha}, t). \tag{D2}$$

We define the function $r(\boldsymbol{x}, \boldsymbol{k}, t)$ by

$$r(\boldsymbol{x}, \boldsymbol{K}(\boldsymbol{x}, \boldsymbol{\alpha}, t), t) = -\delta\theta(\boldsymbol{x}, \boldsymbol{\alpha}, t). \tag{D3}$$

Taking the variation at fixed $\boldsymbol{\alpha}$ of the second equation in (D2) and using (D3) gives

$$\delta\omega = \partial_t r + \partial_t \boldsymbol{K} \cdot \boldsymbol{\nabla}_{\boldsymbol{k}} r - \delta\boldsymbol{K} \cdot \boldsymbol{\nabla}_{\boldsymbol{k}}\omega. \tag{D4}$$

On the other hand, the variation and time derivative of the first of (D2) give

$$\delta\boldsymbol{K} = -\boldsymbol{\nabla}_{\boldsymbol{x}} r - \boldsymbol{\nabla}_{\boldsymbol{x}}\boldsymbol{K} \cdot \boldsymbol{\nabla}_{\boldsymbol{k}} r, \tag{D5a}$$

$$\partial_t \boldsymbol{K} = -\boldsymbol{\nabla}_{\boldsymbol{x}}\omega - \boldsymbol{\nabla}_{\boldsymbol{x}}\boldsymbol{K} \cdot \boldsymbol{\nabla}_{\boldsymbol{k}}\omega, \tag{D5b}$$

where the contractions are between $\boldsymbol{K}$ and $\boldsymbol{\nabla}_{\boldsymbol{k}}$. Introducing (D5) into (D4) and using that $\boldsymbol{\nabla}_{\boldsymbol{x}}\boldsymbol{K} = \boldsymbol{\nabla}_{\boldsymbol{x}}\boldsymbol{\nabla}_{\boldsymbol{x}}\theta$ is a symmetric tensor leads to expression (4.25) for $\delta\omega$.

References

Abrashkin, A.A. & Pelinovsky, E.N. 2017 Lagrange form of the nonlinear Schrödinger equation for low-vorticity waves in deep water. *Nonlinear Proc. Geophys.* **24**, 255–264.

Abrashkin, A.A. & Pelinovsky, E.N. 2018 Dynamics of a wave packet on the surface of an inhomogeneously vortical fluid (Lagrangian description). *Izvestiya, Atmos. Oceanic Phys.* **54**, 101–105.

Andrews, D.G. & McIntyre, M.E. 1978 An exact theory of nonlinear waves on a Lagrangian-mean flow. *J. Fluid Mech.* **89** (04), 609–646.

Ardhuin, F., Rascle, N. & Belibassakis, K.A. 2008 Explicit wave-averaged primitive equations using a generalized Lagrangian mean. *Ocean Model.* **20** (1), 35–60.

Banihashemi, S. & Kirby, J.T. 2019 Approximation of wave action conservation in vertically sheared mean flows. *Ocean Model.* **143**, 101460.

Banihashemi, S., Kirby, J.T. & Dong, Z. 2017 Approximation of wave action flux velocity in strongly sheared mean flows. *Ocean Model.* **116**, 33–47.

Breivik, Ø., Mogensen, K., Bidlot, J.-R., Balmaseda, M.A. & Janssen, P.A.E.M. 2015 Surface wave effects in the NEMO ocean model: forced and coupled experiments. *J. Geophys. Res.: Oceans* **120** (4), 2973–2992.

Bretherton, F.P. 1970 A note on Hamilton's principle for perfect fluids. *J. Fluid Mech.* **44**, 19–31.

Bretherton, F.P. 1971 The general linearized theory of wave propagation. In *Mathematical Problems in the Geophysical Sciences, Lectures in Applied Mathematics* (ed. W.H. Reid), vol. 13, pp. 61–102. American Mathematical Society.

Bretherton, F.P. & Garrett, C.J.R. 1968 Wavetrains in inhomogeneous moving media. *Proc. R. Soc. Lond. Ser. A. Math. Phys. Sci.* **302** (1471), 529–554.

Clementi, E., Oddo, P., Drudi, M., Pinardi, N., Korres, G. & Grandi, A. 2017 Coupling hydrodynamic and wave models: first step and sensitivity experiments in the Mediterranean Sea. *Ocean Dyn.* **67**, 1293–1312.

Couvelard, X., Lemarié, F., Samson, G., Redelsperger, J.-L., Ardhuin, F., Benshila, R. & Madec, G. 2020 Development of a two-way-coupled ocean–wave model: assessment on a global NEMO (v3. 6)–WW3 (v6. 02) coupled configuration. *Geosci. Model Develop.* **13** (7), 3067–3090.

https://doi.org/10.1017/jfm.2026.12065 Published online by Cambridge University Press

CRAIK, A.D.D. & LEIBOVICH, S. 1976 A rational model for Langmuir circulations. *J. Fluid Mech.* **73** (03), 401–426.
CZESCHEL, L. & EDEN, C. 2023 Energy transfers in surface wave-averaged equations. arXiv:2311.13354.
DEWAR, R.L. 1970 Interaction between hydromagnetic waves and a time-dependent, inhomogeneous medium. *Phys. Fluids* **13** (11), 2710–2720.
GALLET, B. & YOUNG, W.R. 2014 Refraction of swell by surface currents. *J. Mar. Res.* **72**, 105–126.
GILBERT, A.D. & VANNESTE, J. 2018 Geometric generalised Lagrangian mean theories. *J. Fluid Mech.* **839**, 95–134.
GILBERT, A.D. & VANNESTE, J. 2025 Geometric approaches to Lagrangian averaging. *Annu. Rev. Fluid Mech.* **57**, 117–140.
GJAJA, I. & HOLM, D.D. 1996 Self-consistent Hamiltonian dynamics of wave mean-flow interaction for a rotating stratified incompressible fluid. *Phys. D: Nonlinear Phenom.* **98** (2), 343–378.
GRIMSHAW, R. 1984 Wave action and wave-mean flow interaction, with application to stratified shear flows. *Annu. Rev. Fluid Mech.* **16**, 11–44.
HASSELMANN, K. 1970 Wave-driven inertial oscillations. *Geophys. Astrophys. Fluid* **1** (3–4), 463–502.
HELL, M., FOX-KEMPER, B. & CHAPRON, B. 2025 A particle-in-cell wave model for efficient sea-state and swell estimates in Earth System Models – PiCLES. *J. Adv. Model. Earth Syst.* **17**, e2025MS00522.
HOLM, D.D. 1996 The ideal Craik–Leibovich equations. *Phys. D: Nonlinear Phenom.* **98** (2), 415–441.
HOLM, D.D., HU, R. & STREET, O.D. 2023 Lagrangian reduction and wave mean flow interaction. *Physica D* **454**, 133847.
HOLM, D.D., MARSDEN, J.E. & RATIU, T.S. 1998 The Euler–Poincaré equations and semidirect products with applications to continuum theories. *Adv. Maths* **137**, 1–81.
HOLTHUIJSEN, L.H. 2010 *Waves in Oceanic and Coastal Waters*. Cambridge University Press.
HUANG, N.E. 1979 On surface drift currents in the ocean. *J. Fluid Mech.* **91** (1), 191–208.
JANSSEN, P. 2004 *The Interaction of Ocean Waves and Wind*. Cambridge University Press.
KIRBY, J.T. & CHEN, T.-M. 1989 Surface waves on vertically sheared flows: approximate dispersion relations. *J. Geophys. Res.: Oceans* **94** (C1), 1013–1027.
KOMEN, G.J., CAVALERI, L., DONELAN, M., HASSELMANN, K., HASSELMANN, S. & JANSSEN, P.A.E.M. 1996 *Dynamics and Modelling of Ocean Waves*. Cambridge University Press.
LEIBOVICH, S. 1980 On wave-current interaction theories of Langmuir circulations. *J. Fluid Mech.* **99** (04), 715–724.
MCINTYRE, M.E. 1981 On the wave momentum myth. *J. Fluid Mech.* **106**, 331–347.
MCINTYRE, M.E. 1988 A note on the divergence effect and the Lagrangian-mean surface elevation in periodic water waves. *J. Fluid Mech.* **189**, 235–242.
MCWILLIAMS, J.C. 2022 *Quasi-Linear Theory for Surface Wave-Current Interactions*. Springer.
MCWILLIAMS, J.C., RESTREPO, J.M. & LANE, E.M. 2004 An asymptotic theory for the interaction of waves and currents in coastal waters. *J. Fluid Mech.* **511**, 135–178.
MCWILLIAMS, J.C., SULLIVAN, P.P. & MOENG, C.-H. 1997 Langmuir turbulence in the ocean. *J. Fluid Mech.* **334**, 1–30.
NEWCOMB, W.A. 1962 Lagrangian and Hamiltonian methods in magnetohydrodynamics. *Nucl. Fusion* (Supplement Part 2), **2**, 451–463.
PIZZO, N., LENAIN, L., RØMCKE, O., ELLINGSEN, S.Å. & SMELTZER, B.K. 2023 The role of Lagrangian drift in the geometry, kinematics and dynamics of surface waves. *J. Fluid Mech.* **954**, R4.
PIZZO, N. & SALMON, R. 2021 Particle description of the interaction between wave packets and point vortices. *J. Fluid Mech.* **925**, A32.
PORCILE, G., BENNIS, A.-C., BOUTET, M., LE BOT, S., DUMAS, F. & JULLIEN, S. 2024 Implementation of additional spectral wave field exchanges in a three-dimensional wave–current coupled WAVEWATCH-III (version 6.07) and CROCO (version 1.2) configuration: assessment of their implications for macro-tidal coastal hydrodynamics. *Geosci. Model Develop.* **17** (7), 2829–2853.
RESSEGUIER, V., HASCOËT, E. & CHAPRON, B. 2024 Wave propagation in random two-dimensional turbulence: a multiscale approach. *J. Fluid Mech.* **997**, A51.
SALMON, R. 1988 Hamiltonian fluid mechanics. *Annu. Rev. Fluid Mech.* **20** (1), 225–256.
SALMON, R. 2016 Variational treatment of inertia–gravity waves interacting with a quasi-geostrophic mean flow. *J. Fluid Mech.* **809**, 502–529.
SALMON, R. 2020 *More Lectures on Geophysical Fluid Dynamics*. Available at: http://pordlabs.ucsd.edu/rsalmon/More.Lectures.pdf.
SESHASAYANAN, K. & GALLET, B. 2019 Surface gravity waves propagating in a rotating frame: the Ekman–Stokes instability. *Phys. Rev. Fluids* **4** (10), 104802.

https://doi.org/10.1017/jfm.2026.12065 Published online by Cambridge University Press

SKYLLINGSTAD, E.D. & DENBO, D.W. 1995 An ocean large-eddy simulation of Langmuir circulations and convection in the surface mixed layer. *J. Geophys. Res.: Oceans* **100** (C5), 8501–8522.

SOWARD, A.M. & ROBERTS, P.H. 2010 The hybrid Euler–Lagrange procedure using an extension of Moffatt's method. *J. Fluid Mech.* **661**, 45–72.

STEWART, R.H. & JOY, J.W. 1974 HF radio measurements of surface currents. *Deep Sea Res. Oceanogr. Abstr.* **21** (12), 1039–1049.

SUN, R., COBB, A., VILLAS BÔAS, A.B., LANGODAN, S., SUBRAMANIAN, A.C., MAZLOFF, M.R., CORNUELLE, B.D., MILLER, A.J., PATHAK, R. & HOTEIT, I. 2023 Waves in SKRIPS: WAVEWATCH III coupling implementation and a case study of tropical cyclone Mekunu. *Geosci. Model Develop.* **16** (12), 3435–3458.

SUZUKI, N. & FOX-KEMPER, B. 2016 Understanding Stokes forces in the wave-averaged equations. *J. Geophys. Res.: Oceans* **121** (5), 3579–3596.

TAKENS, F. 1980 Motion under the influence of a strong constraining force. In *Global Theory of Dynamical Systems: Proceedings of an International Conference Held at Northwestern University, Evanston, Illinois, June 18-22, 1979* (ed. Z. Nitecki & C. Robinson), pp. 425–445. Springer.

URSELL, F. & DEACON, G.E.R. 1950 On the theoretical form of ocean swell on a rotating earth. *Geophys. J. Intl* **6**, 1–8.

VANNESTE, J. & YOUNG, W.R. 2022 Stokes drift and its discontents. *Phil. Trans. R. Soc. A* **380** (2225), 20210032.

VILLAS BÔAS, A.B., CORNUELLE, B.D., MAZLOFF, M.R., GILLE, S.T. & ARDHUIN, F. 2020 Wave-current interactions at meso and submesoscales: insights from idealized numerical simulations. *J. Phys. Oceanogr.* **50** (12), 3483–3500.

VILLAS BÔAS, A.B. & YOUNG, W.R. 2020 Directional diffusion of surface gravity wave action by ocean macroturbulence. *J. Fluid Mech.* **890**, R3.

WAGNER, G.L., CHINI, G.P., RAMADHAN, A., GALLET, B. & FERRARI, R. 2021 Near-inertial waves and turbulence driven by the growth of swell. *J. Phys. Oceanogr.* **51** (5), 1337–1351.

WAGNER, G.L., PIZZO, N., LENAIN, L. & VERON, F. 2023 Transition to turbulence in wind-drift layers. *J. Fluid Mech.* **976**, A8.

WANG, H., VILLAS BÔAS, A.B., VANNESTE, J. & YOUNG, W.R. 2025 Scattering of surface waves by ocean currents: the U2H map. *J. Fluid Mech.* **1005**, A12.

WANG, H., VILLAS BÔAS, A.B., YOUNG, W.R. & VANNESTE, J. 2023 Scattering of swell by currents. *J. Fluid Mech.* **975**, A1.

WHITE, B.S. & FORNBERG, B. 1998 On the chance of freak waves at sea. *J. Fluid Mech.* **355**, 113–138.

WHITHAM, G.B. 1965 A general approach to linear and nonlinear dispersive waves using a Lagrangian. *J. Fluid Mech.* **22**, 135–147.

WHITHAM, G.B. 1974 *Linear and Nonlinear Waves*. Wiley.

XIE, J.-H. & VANNESTE, J. 2015 A generalised-Lagrangian-mean model of the interactions between near-inertial waves and mean flow. *J. Fluid Mech.* **774**, 143–169.

https://doi.org/10.1017/jfm.2026.12065 Published online by Cambridge University Press